Main text

Diverse gut pathogens exploit the host engulfment pathway via a conserved mechanism

AUTHORS:
Mahitha Shree Anandachar[1,2], Suchismita Roy[1], Saptarshi Sinha[1], Agyekum Boadi[1], Stella-Rita Ibeawuchi[2], Hobie Gementera[2], Alicia Amamoto[2], Gajanan D. Katkar[1]* and Pradipta Ghosh[1, 3]*

AFFILIATIONS:
[1]*Department of Cellular and Molecular Medicine, University of California San Diego.*
[2]*Department of Pathology, University of California San Diego.*
[3]*Department of Medicine, University of California San Diego.*

RUNNING TITLE: Gut pathogens exploit host's engulfment pathway

***CORRESPONDING AUTHORS:**

Gajanan D. Katkar, Ph.D.; Departments of Cellular and Molecular Medicine, University of California San Diego, CA 92093. **Phone**: 858-346-3507: **Email:** kgajanandattatray@ucsd.edu

Pradipta Ghosh, M.D.; Professor, Departments of Medicine and Cellular and Molecular Medicine, University of California San Diego, CA 92093. **Phone**: 858-822-7633: **Email:** prghosh@ucsd.edu

GRAPHICAL ABSTRACT

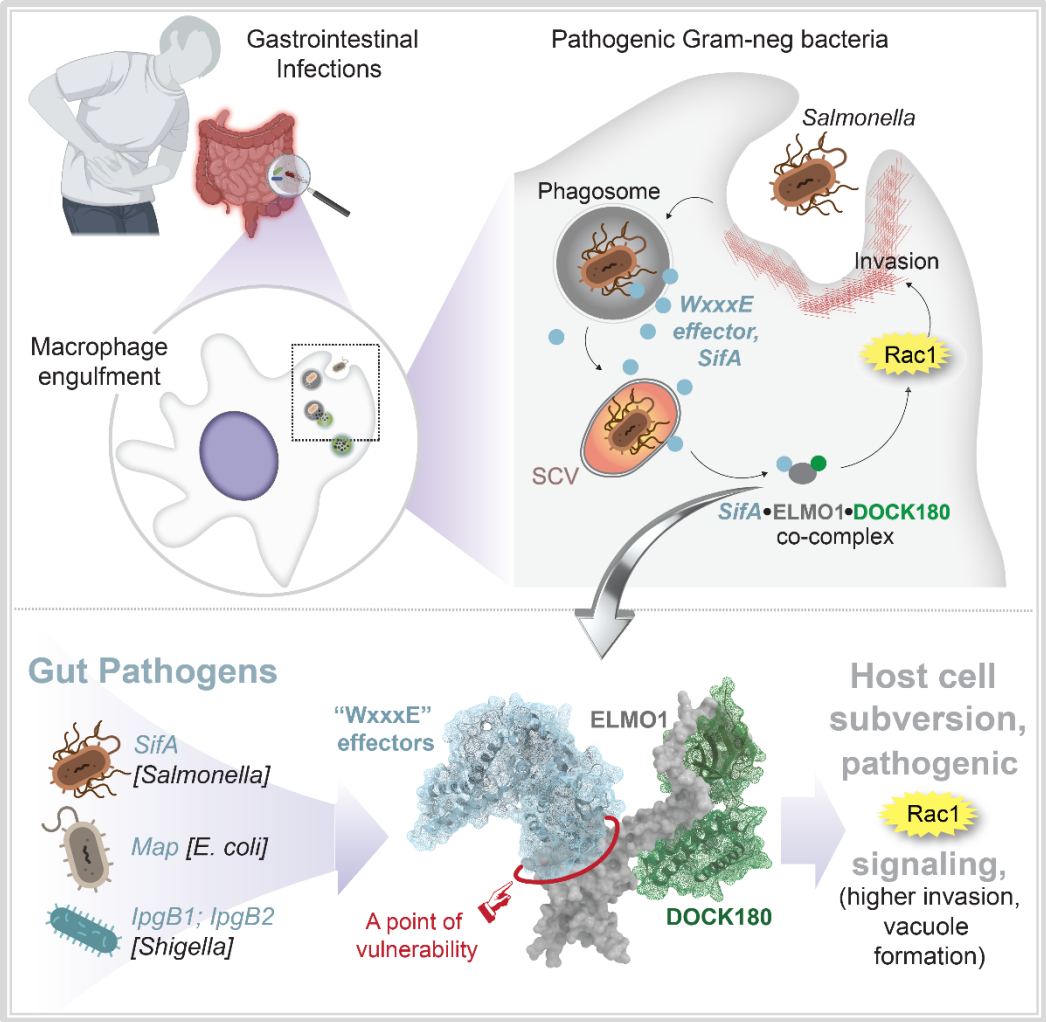

In brief: This work defines the nature of a conserved molecular interface, assembled between diverse W*xxxE* motif-containing effector proteins encoded by gut pathogens and the host innate immune sensor, ELMO1, via which pathogens exploit the host's engulfment machinery.

ABSTRACT

Macrophages clear infections by engulfing and digesting pathogens within phagolysosomes. Pathogens escape this fate by engaging in a molecular arms race; they use *WxxxE* motif-containing "effector" proteins to subvert the host cells they invade and seek refuge within protective vacuoles. Here we define the host component of the molecular arms race as an evolutionarily conserved polar 'hotspot' on the PH-domain of ELMO1 (*E*ngu*l*fment and Cell *Mo*tility1), which is targeted by diverse *WxxxE*-effectors. Using homology modeling and site-directed mutagenesis, we show that a lysine triad within the 'patch' directly binds all *WxxxE*-effectors tested: SifA (*Salmonella)*, IpgB1 and IpgB2 (*Shigella*), and Map (enteropathogenic *E. coli*). Using an integrated SifA•host protein-protein interaction (PPI) network, *in-silico* network perturbation, and functional studies we show that the major consequences of preventing SifA•ELMO1 interaction are reduced Rac1 activity and microbial invasion. That multiple effectors of diverse structure, function, and sequence bind the same hotpot on ELMO1 suggests that the *WxxxE*-effector(s)•ELMO1 interface is a convergence point of intrusion detection and/or host vulnerability. We conclude that the interface may represent the fault line in co-evolved molecular adaptations between pathogens and the host and its disruption may serve as a therapeutic strategy.

KEY WORDS:

ELMO1, Rac1, Dock180, *SifA, Engulfment, Salmonella, WxxxE*-effectors

INTRODUCTION

Enteric pathogens such as *Salmonella* rely upon their virulence factors to invade and replicate within host cells. Upon invasion, they seek refuge within a modified phagosome-like structure, the *Salmonella*-containing vacuole (SCV) (1), within which they survive, even replicate, or simply persist in a dormant-like state (2). Both invasion and SCV formation require the delivery of microbial effector proteins via Type III Secretion Systems (T3SSs) into the host cell; they both require the cooperation of a subverted host cell whose phagolysosomal signaling and membrane trafficking pathways are manipulated to mount very dynamic and extensive membrane remodeling and actin rearrangement (1). Thus, three key aspects facilitating *Salmonella* pathogenesis are (i) vacuole formation for refuge, (ii) delivery of effector proteins via T3SSs to interfere and/or manipulate the host system, facilitating (iii) more bacterial invasion. These mechanisms of pathogenesis are shared also among other enteric pathogens such as enteropathogenic *E. coli* EHECs, EPECs, and *Shigella*. *E. coli* rely upon T3SS effectors--e.g., Map, EspH, and EspF--to form *E. coli*-containing vacuoles (ECVs) (3) and manipulate the host cell form pedestals (4), filopodia, or microspikes for invasion, whereas *Shigella* rely upon T3SS effectors, e.g., IpgB1/2, to form vacuoles (5) and manipulate host cells into forming membrane ruffles for orchestrating what is known as "the trigger mechanism of entry" (6-9). Similar mechanisms are also used by *Yersinia* (10) and *Campylobacter* (11) to subvert host epithelial cells.

Regardless of the diversity of the pathogens, their equally diverse T3SS injectosomes, or the repertoire of effectors (reviewed in (12)), the host actin cytoskeleton has emerged as the dynamic hub in a microbe-induced circuitry of Ras-superfamily GTPases [Ras homolog family member A (RhoA), Ras-related C3 botulinum toxin substrate 1 (Rac1) and Cell division control (Cdc) protein-42] (13). Diverse microbes converge upon and exploit the host circuitry to mount pathogenic signaling, escape lysosomal clearance by seeking refuge in vacuoles, invade host cells and alter inflammatory response. As for mechanism(s) for such convergence, the ability of a *WxxxE* motif-containing family of effectors to directly activate host GTPases was reported first (14). By activating host Rho GTPases, the WxxxE effectors subvert actin dynamics (15). SopE, IpgB1 and EspT trigger membrane ruffles (16-18), IpgB2 and EspM trigger stress fibers (19) and Map trigger filopodia (20) via activation of Rac1, RhoA and Cdc42 respectively. Engulfment and cell Motility protein 1 (ELMO1) was identified subsequently as a *WxxxE* effector-interacting host protein (21). Three independent groups, each using ELMO1-knockout animals that were infected with different pathogens (*Shigella (6)*, *Salmonella* (21)and *E. coli* (22)), have implicated the *WxxxE*•ELMO1 interaction in the augmentation of the actin•GTPase circuitry via the well-established ELMO1•DOCK180 (Dedicator of cytokinesis)→Rac1 axis (23-25). Within this signaling cascade, ELMO1•Dock180 is a bipartite guanine nucleotide exchange factor (GEF) for the monomeric GTPase Rac1 (26), but is also capable of activating Cdc42 (27) and RhoA (28).

Despite these insights, key questions remained unanswered, e.g., how do the *WxxxE*-effectors, which are unique to gut pathogens (21) (yet to be found in commensals (29)) converge on one host macro-molecular complex (the ELMO1•Dock180→RhoGTPases) to subvert host actin dynamics. Because the *WxxxE*-effectors are structurally and functionally diverse except for the *WxxxE*-motif, which is their defining and unifying feature, initial studies hypothesized that this motif could be the mechanism of such convergence; but four structural studies revealed otherwise (26, 30-32). These studies of SifA, IpgB, and Map structures and

a EspM2 model showed that Trp (W) and Glu (E) within the *WxxxE*-motif are ‘structural residues’ that are positioned around the junction of the two 3-α-helix bundles and maintain the conformation of a ‘catalytic loop’ through hydrophobic contacts with surrounding residues. Consistent with these conclusions, conserved substitutions (W→Y and E→D; in EpsM (19)) did not alter stability or functions, whereas W→A or E→A substitutions make the protein highly unstable (33) and render it non-functional (34). With the *WxxxE*-motif ‘ruled out’ as the potential contact site for convergence, the basis for how diverse *WxxxE*-effectors may bind ELMO1 and induce convergent pathogenic signaling via the ELMO1•DOCK axis remains unknown. Using a transdisciplinary and multi-scale approach that spans structural models as well as protein-protein interaction networks, here we reveal a surprisingly conserved molecular mechanism for how diverse pathogens use their *WxxxE*-effectors to hijack the ELMO1•DOCK•Rac1 axis via a singular point of vulnerability on ELMO1.

RESULTS AND DISCUSSION

ELMO1 and SifA *cooperate during vacuole formation.*

Prior work has separately implicated both ELMO1(35) and SifA (32, 36, 37) in *Salmonella* pathogenesis. While SifA has been directly implicated in the formation of SCVs (32, 37), ELMO1 was shown to impact bacterial colonization, dissemination, and inflammatory cytokines *in vivo* (21). We asked if both proteins are required for SCV formation. We stably depleted ELMO1 in J774 macrophages by short hairpin (sh)RNA (>99% depletion compared to controls; **Figure 1A**), infected them with either the WT (SL) or a mutant *Salmonella* strain that lacks *SifA* (*ΔSifA*), and then assessed the ultrastructure of the SCVs by transmission electron microscopy (TEM) (see workflow; **Figure 1B**). Bacteria were observed as either intact within vacuoles, free in cytosol, or partially digested within fused lytic compartments, as reported previously (38) (**Figure 1C-D**). When assessed for the completeness of the vacuolar wall (see basis for quantification; **Figure 1E**), WT *Salmonella* formed complete SCVs at a significantly lower rate in ELMO-depleted macrophages compared to controls (13% vs 35%; **Figure 1F, H**). Absence of SifA impaired SCV biogenesis regardless of the presence or absence of ELMO1 (**Figure 1G, H**). Findings demonstrate that both ELMO1 and SifA are required for SCV formation and suggest cooperativity between the two proteins during SCV biogenesis.

SifA *directly binds the C-terminus of ELMO1.*

We next asked if SifA binds ELMO1; the latter is a multi-modular protein with several known interacting partners (summarized in **Figure 1I**). We compared head-to-head equimolar amounts of GST-tagged full length vs. a C-terminal fragment (aa 482-727) of ELMO1 [which contains a pleckstrin-like homology domain (PHD)-; **Figure 1I**] for their ability of to bind a His-tagged recombinant SifA protein. The C-terminal PH-domain was prioritized because of two reasons: (i) A recent domain mapping effort using fragments of ELMO1 on cell lysates expressing SifA had ruled out contributions of the N-terminal domain in mediating this interaction (21); and (ii) SifA directly binds another PH-domain, SKIP, forming 1:1 complex at micromolar dissociation constant, the structural basis for which has been resolved (26, 39). We found that both full length ELMO1 and its C-terminal fragment can bind His-SifA (**Figure 1J**). Binding was also observed when the bait and prey proteins were swapped, such that immobilized GST-SifA was tested for its ability to bind His-ELMO1 proteins (**Figure 1K**). Because interactions occurred between recombinant proteins purified to >95% purity, we conclude that the SifA•ELMO1 interaction is direct. Because SifA bound both the full length and the C-terminal fragment of ELMO1 to a similar extent, we conclude that the C-terminus of ELMO1 is sufficient for the interaction.

SifA *binds to an evolutionarily conserved lysine hotspot on ELMO1's PH domain.*

To gain insights into the nature of the SifA•ELMO1 interface, we leveraged two previously resolved structures of a SifA•SKIP-PHD co-complex (32) and ELMO1-PHD to build a homology model of SifA•ELMO1-PHD complex (see **Fig.S1** for workflow and *Methods*). The resultant model helped draw three key important conclusions: (i) the resolved structure of SifA•SKIP (32) and the model for SifA•ELMO1 were very similar, and hence, the specific recognition of SifA by both SKIP-PHD and ELMO1-PHD was predicted to be mediated through a large network of contacts (**Figure 2A**), primarily electrostatic in nature (**Fig.S1C-D**); (ii) the

tryptophan (W197, deeply buried within the hydrophobic core of SifA) and glutamate (E201) within the *WxxxE*-motif (red residues; **Fig. S2**), which are essential for protein stability, but dispensable for binding SKIP (26) are likely to be nonessential also for ELMO1; and (iii) the amino acids deemed essential for the assembly of the SifA•ELMO1 interface were: a pair of hydrophobic residues, Leucine (L)130 and Methionine (M)131 on SifA and a triad of polar lysine residues within the β5-β6 loop of ELMO1 (K620, K626 and K628) (**Figure 2A-B**). An alignment of the sequences of ELMO1-PHD and SKIP-PHD showed the lysine triad in ELMO1 corresponds to the corresponding contact sites on SKIP for SifA in the resolved complex(26) (**Figure 2C**; **Fig. S3A**). A full catalog of both inter- and intramolecular contact sites (see **Supplemental Information 1**) revealed how each lysine within the lysine triad in the β5-β6 loop of ELMO1 contributes uniquely to generate the electrostatic attractions that stabilize the SifA•ELMO1 complex (**Figure 2B**): (i) K628 primarily establishes intermolecular electrostatic contacts with L130 and M131 on SifA; (ii) K626 mediates intermolecular interaction by engaging K132 and also via charge-neutralizing salt-bridges with Asp(D)117 on SifA. It also mediates intramolecular interactions with D621 within the β5-β6 loop of ELMO1; (iii) K620 primarily engages in intramolecular contact with two other residues within the β5-β6 loop, L631 and L638, thus stabilizing the loop. Thus, all 3 lysines within the triad appeared important: While K628 and K626 establish strong electrostatic interactions with SifA, K626 and K620 stabilize the β5-β6 loop that contains the lysine triad.

We noted that K620 is reported to be ubiquitinated and the Threonine (T) at 618 is phosphorylated (**Fig. S3B**); none of the lysine residues are reported to be impacted by germline SNPs or somatic mutations in cancers. Most importantly, the β5-β6 loop and the lysine triad within this stretch, are evolutionarily conserved from fish to humans, as well as in the homologous members of the family, ELMO2 and ELMO3 (**Figure 2D**; **Fig. S4**).

To analyze the electrostatics for the model of the SifA•ELMO1 complex, we used APBS (Adaptive Poisson-Boltzmann Solver) (40), a widely accepted software for solving the equations of continuum electrostatics for large biomolecular assemblages. We found that in the most energetically favorable orientation, charged residues Lys(K)628 and Lys(K)626 on ELMO1 bring hydrophobic residues Met(M)131 and Leu(L)130 on SifA into proximity (**Figure 2E**; **Fig. S5**). Because the APBS approach allows us to determine the electrostatic interaction profile as a function of the distance between two molecules, we conclude that the lysines K628 and K626, and potentially other amino acids in the β5-β6 loop are key sites on ELMO1 that engage in electrostatic interactions with L130 and M131 on SifA.

We validated the homology model and the nature of the major interactions [i.e., electrostatic] in the assembly of the complex by generating several structure-rationalized mutants of ELMO1 and SifA. The positively charged lysines on ELMO1 were substituted with negatively charged aspartate residues (D; ELMO1-CT-K3D), expecting that such substitution will disrupt the intermolecular electrostatic attractions and destabilize the SifA•ELMO1 complex. These substitutions were expected to also disrupt intramolecular interactions within the β5-β6 loop (**Figure 2D**) and destabilize the highly conserved loop. The hydrophobic residues on SifA, i.e., L130 and M131, were substituted with an unfavorable negatively charged and polar aspartate residue, either alone (L130D; M131D) or in combination (LM>DD). Binding to SifA was significantly reduced in the case of the K3D ELMO1 mutant (**Figure 2F-G**), and binding to ELMO1 was virtually abolished in the case of all the SifA mutants (**Figure 2H**).

Although both L130 and M131 on SifA were predicted to bind ELMO1, L130 was predicted to be the major contributor (accounting for 13 of the 17 intermolecular contact sites; **Supplemental Information 1**). M131, on the other hand, engaged also in numerous *intra*molecular contacts, which suggests that M131 could be important also for protein conformation. We asked if the strong polar contacts between L130(SifA) and the lysine triad (ELMO1) were critical for the SifA•ELMO1 interaction (**Figure 2B**) and tested their relative contributions without disrupting M131(SifA). Pulldown assays showed that SifA•ELMO1 interactions were partially impaired when L130D-SifA and K3D-ELMO1 substitutions when used alone (**Figure 2I-J**) and virtually lost when the mutants were used concomitantly (**Figure 2I-J**).

These findings provide atomic level insights into the nature and composition of the SifA•ELMO1 complex which is assembled when a pair of hydrophobic residues on SifA binds an evolutionarily conserved polar hot spot on ELMO1-PHD. Strong hydrophobic interactions stabilize the SifA•ELMO1 interface which can be selectively disrupted.

Disrupting the SifA•ELMO1 interface suppresses Rac1 activity and bacterial invasion.

To assess the impact of selective disruption of the SifA•ELMO1 interface in the setting of an infection, we used an unbiased network-based approach. We leveraged a previously published (41) SifA interactome, as determined by proximity-dependent biotin labelling (BioID) and used those interactors as 'seeds' for fetching additional interactors to build an integrated SifA(*Salmonella*)•host PPI network (see *Methods* for details). The resultant network (**Fig. S6A**) was perturbed by *in-silico* deletion of either ELMO1 (**Figure 3A, Fig. S6B**) or, more specifically, the SifA•ELMO1 interaction (**Figure 3B**). Both modes of perturbation were analyzed by a differential network analysis (with *vs*. without perturbations) using various network metrices (see legends; **Figure 3C, E**). As one would expect, deletion of ELMO1 impacts many proteins (**Figure 3C**; **Fig. S6C-D**), including those engaged in microbe sensing (BAI1, NOD1, NOD2), membrane trafficking along the phagolysosomal pathway (EEA1, Rab5A, Rab9A and LAMP), multiple Src-family kinases (LYN, YES and HCK), inflammatory cytokines (IL1B, CCL2/MCP1, CXCL12, and TNF), as well as immune cell (B cell) and epithelial (adherens junction) pathways (**Figure 3D**). Findings are consistent with prior published work, implicating ELMO1 in facilitating the recruitment of LAMP1 to SCVs (42), mounting a cytokine response (21, 35), as well as regulating epithelial junctions (43) upon *Salmonella* infection. The proteins found to be impacted based on at least two network metrices (**Figure 3C**) are enriched for Rac1 signaling (Rac1, Rac2, Nckap1 and Dok180) and the endolysosomal pathway (LAMP and RABs). The more refined approach of selective deletion of the SifA•ELMO1 interaction yielded, as expected, a smaller list of proteins that mostly concerned with the DOCK1•RAC signaling axis and Src family kinases, HCK, LYN and YES (**Figure 3E-F**). Because phosphorylation of ELMO1 by Src-family kinases such as Src, Fyn (44), and HCK (45) also converge on Rac1 activity, Rac1 signaling, likely via the ELMO1•DOCK1 axis, emerged as the most important function predicted to be impacted in infected cells.

Structure homology models of ternary complexes of SifA•ELMO1•DOCK revealed that although both SifA and DOCK180 bind ELMO1-PHD, they do so via two distinct and non-overlapping interfaces (**Figure 3G**). To experimentally validate this finding, we generated a mutant ELMO1 (W665A) that was previously

confirmed by two independent groups to be essential for binding DOCK180 (46, 47) and tested its ability to bind His-SifA in pulldown assays. Both WT and ELMO1-W665A bound SifA to similar extents, indicating that W665 is dispensable for binding SifA (**Figure 3H**). Findings are also consistent with the fact that both SifA and DOCK180 co-immunoprecipitate with ELMO1 (21), and hence, may exist as a ternary complex.

We anticipated that selective disruption of the SifA•ELMO1 interface (using the ELMO1-K3D mutant), while leaving intact the ELMO1•DOCK interface, would interrupt the ELMO1•DOCK•Rac1 signaling axis and reduce bacterial invasion (**Figure 3I-J)**. This was indeed found to be the case as Rac1 signaling was induced during *Salmonella* infection in ELMO1-depleted J774 macrophages reconstituted with WT ELMO1 but found to be significantly blunted when the same macrophages were reconstituted with the K3D mutant ELMO1 (**Figure 3K-L**). Reduced Rac1 activity was also associated with reduced bacterial internalization (**Figure 3M**). Findings demonstrate that one of the major consequences of mutating the polar triad of lysine residues on ELMO1 is reduction in both Rac1 activity and microbial invasion.

Diverse WxxxE-effectors target the same lysine hotspot on ELMO1.

Prior work using ELMO1-*knockout* zebrafish (*E. coli*/MAP (22)) and mouse (*Shigella*/IpgB1 (6) and *Salmonella*/*SifA*) (21) have independently concluded that diverse pathogens trigger host immune responses via *interaction with* ELMO1. We asked if our insights into the nature of the SifA•ELMO1 interface are relevant also to other *WxxxE* motif-containing effectors. As observed previously for SifA (**Figure 1J-K**), *WxxxE*-effectors IpgB1, IpgB2 and Map also directly bound both full length (**Figure 4A**-*top*) and the C-terminal PHD containing fragment (**Figure 4A**-*bottom*) of ELMO1. More importantly, mutation of the polar lysine triad on ELMO1 reduced the binding of all effectors tested (**Figure 4B-C**), indicating that these effectors require the same hotspot as SifA to engage with ELMO1, presumably via similar hydrophobic contacts. Because the effectors have little to no sequence similarity other than the invariant *WxxxE*-motif (see alignment; **Fig. S7**), and the N-terminal extension is unique to SifA, we were unable to predict the exact nature of the potential hydrophobic contacts on the effectors. We conclude that the newly identified hotspot on ELMO1 represents a point of convergence for numerous *WxxxE*-effectors encoded by diverse pathogens to engage with one host protein. It is noteworthy that each of these *WxxxE*-effectors we tested here, have recently been shown to require ELMO1 for inducing Rac1 signaling (21).

CONCLUSIONS AND STUDY LIMITATIONS

This work provides an atomic-level insight into a single point of vulnerability within the host engulfment pathway, i.e., a hot spot (lysine triad) on the ELMO1-PHD. This hot spot is exploited by diverse gut pathogens such as *Salmonella* to activate the ELMO1•DOCK180•Rac1 axis, invade host cells and seek refuge within SCVs (see summary of findings; **Figure 4D**). These findings come as a surprise because the bacterial effector proteins that are responsible for such exploitation are diverse, and yet, they all bind the same hot spot on ELMO1 to hijack the Rac1 axis to their advantage (see legend; **Figure 4E**).

Because the *WxxxE*-motif is found in enteric as well as plant pathogens, and within the Toll/interleukin-1 receptor (TIR) modules of both host and pathogen proteins (but notably absent in commensals (21)), it is possible that some host *WxxxE*-proteins may also engage ELMO1 via the same hot spot. If so, the pathogen-encoded *WxxxE*-effectors should competitively block such interactions, exemplifying the phenomenon of molecular mimicry. The structural insights revealed here also warrants the consideration of another form of competitive binding, one in which the same *WxxxE*-effector (SifA) may bind different host proteins (SKIP or ELMO1) using nearly identical interfaces. Because both interactions require the identical residues on SifA, the SifA•ELMO1 and SifA•SKIP interactions must be mutually exclusive. Given the roles of ELMO1 in the regulation of actin dynamics during bacterial entry and SKIP's role in endosomal tubulation (32) and anterograde movement of endolysosomal compartments (39), we hypothesize that SifA may bind two host proteins sequentially. It may bind ELMO1 first during S*almonella* entry and SCV formation and SKIP later to support cellular processes that help in SCV membrane stabilization, the development of Sifs, and the creation of a favorable environment for the survival and multiplication of *Salmonella* (39, 48). If/how SifA coordinates its interactions with two host proteins, ELMO1 and SKIP, during S*almonella* infection remains unknown; however, the fact that the polar lysine triad on both host proteins is evolutionarily intact from fish to humans suggests that these conserved hot spots on host protein surfaces may have co-evolved with the pathogens as part of a molecular arms race of adaptations. The deleterious impact of structure-rationalized mutants suggests that both the SifA•ELMO1 (shown here) and the SifA•SKIP (published before (26, 32)) interfaces are sensitive to disruption. This is particularly important because hydrophobic interactions that stabilize protein-protein interfaces via a central cluster of hot spot residues are of high therapeutic value because they are amenable to disruption with rationally designed small molecule inhibitors (49).

This study also has few limitations. For example, how post-translational modifications (PTMs) may impact the *WxxxE*•ELMO1 interface was not evaluated. It is possible that lysine methylation, which ironically was described as a PTM first in *Salmonella* flagellin (50), may impact the interface, as shown in other instances (51). Similarly, phosphorylation at T618 or ubiquitination at K620 may have impacts that were not explored; because the ELMO1•DOCK180 co-complex is known to be regulated by ubiquitination (52), and both proteins are downregulated rapidly upon LPS stimulation(53), we speculate that ubiquitination at K621 may deter *WxxxE*-effector interactions and thereby, serve as a protective strategy of the host during acute infections. Finally, the impact of disrupting the *WxxxE*•ELMO1 interface on host immune responses were not

studied here and will require the creation of knock-in K3D mutant models. All these avenues are expected to provide a more complete picture of the consequences of disrupting the *WxxxE*•ELMO1 interface and help formulate strategies to disrupt it for therapeutic purposes.

In conclusion, our studies characterize a polar patch on ELMO1-PHD as a conserved hot spot of host vulnerability—a so-called Achilles heel--which is exploited by multiple pathogens. Because prior studies on ELMO1-*knockout* zebrafish (22) and mice (6, 21) have implicated *WxxxE*•ELMO1 interactions as responsible also for mounting host inflammatory responses, the same polar patch on ELMO1-PHD may also serve as a conserved hot spot of intrusion detection.

FIGURES AND LEGENDS

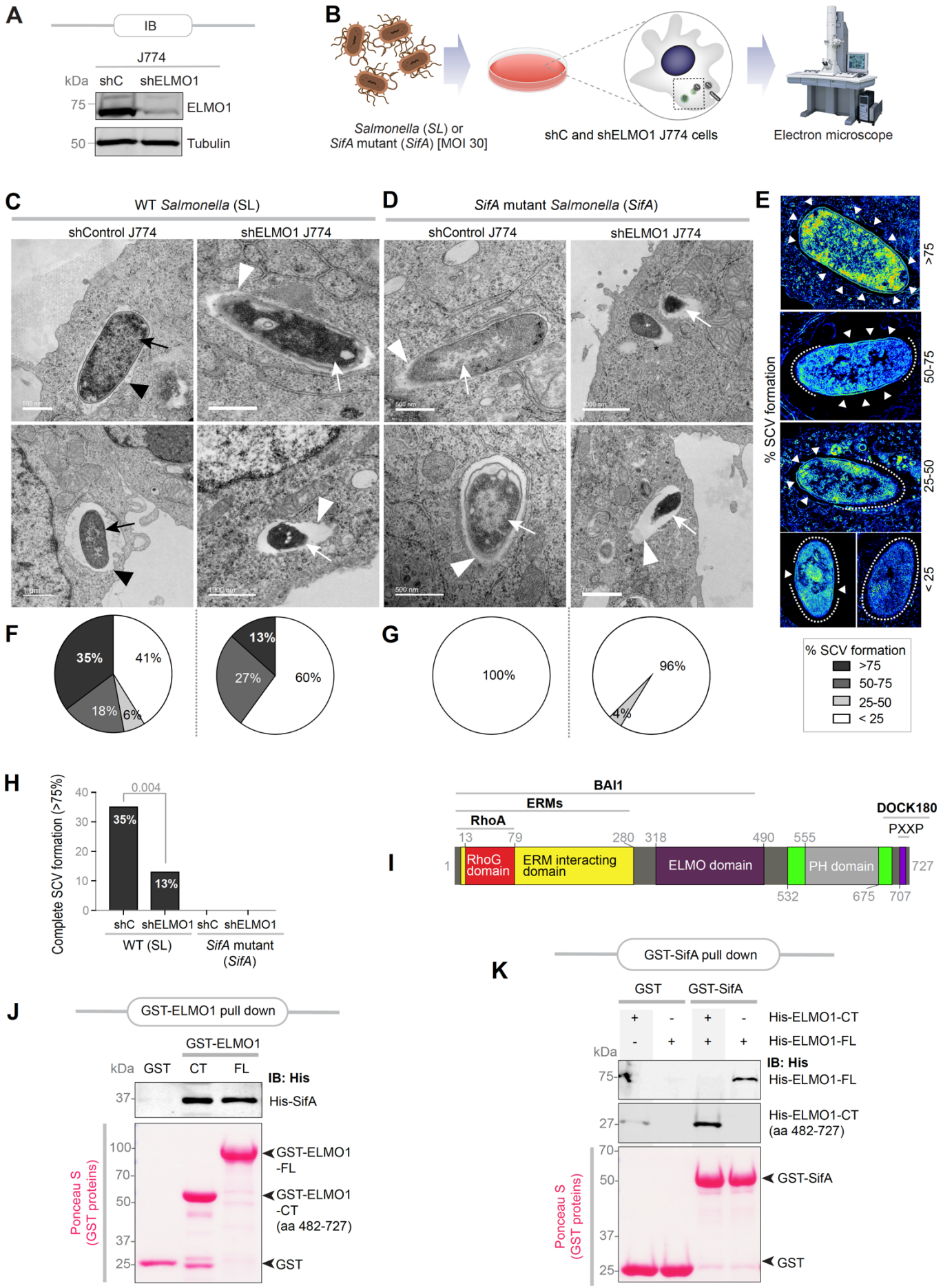

Figure 1: ELMO1 and SifA interact directly and cooperate to promote SCV formation.

A: Immunoblot of control (shC) and ELMO1-depleted (shELMO1) J774 murine macrophages.

B: Schematic shows workflow for TEM on J774 macrophages infected with either *Salmonella* (SL) or a *SifA*-deleted variant strain (SifA) of the same.

C-D: Representative electron micrographs of control (shC) or ELMO1-depleted (shELMO1) J774 macrophages, infected with *S. typhimurium* (SL or *SifA*; 30 moi), at 6 h post-infection. Examples of bacteria within vacuoles (black arrowheads) and cytosolic bacteria (white arrowheads) are indicated. Bacteria that are either Intact (black arrows) or partially degraded upon fusion with lytic compartments (white arrows) are also indicated. Scale bars are placed at the lower left corner of each micrograph.

E-G: A montage (E) of pseudo-colored micrographs of SCVs at various stages of formation is shown. The presence (arrowheads) or absence (interrupted lines) of detectable vacuolar membrane are marked. Pie charts display the percentage of bacteria at each stage of SCV formation (F-G) encountered in C-D.

H: Bar graph display the percentage of complete (representing >75% in E) SCV formation in C-D.

I: A domain map of ELMO1 with major interacting partners. ERM proteins (ezrin, radixin and moesin); PH, pleckstrin homology; BAI1, Brain-specific angiogenesis inhibitor 1 (*ADGRB1*).

J: Recombinant His-SifA (~5 µg) was used in a pulldown assay with immobilized bacterially expressed recombinant GST-tagged full-length (FL) or a C-terminal domain (CT; aa 482-727) of ELMO1 or GST alone (control). Bound SifA was visualized by immunoblot using anti-His (SifA) antibody. GST proteins are visualized by Ponceau S staining.

K: Recombinant His-tagged CT (aa 482-727) or full-length (FL) ELMO1 proteins (~3 µg) were used in a pulldown assay with immobilized bacterially expressed recombinant full-length GST-SifA or GST alone (control). Bound ELMO1 proteins were visualized by immunoblot using anti-His (SifA) antibody. GST proteins are visualized by Ponceau S staining.

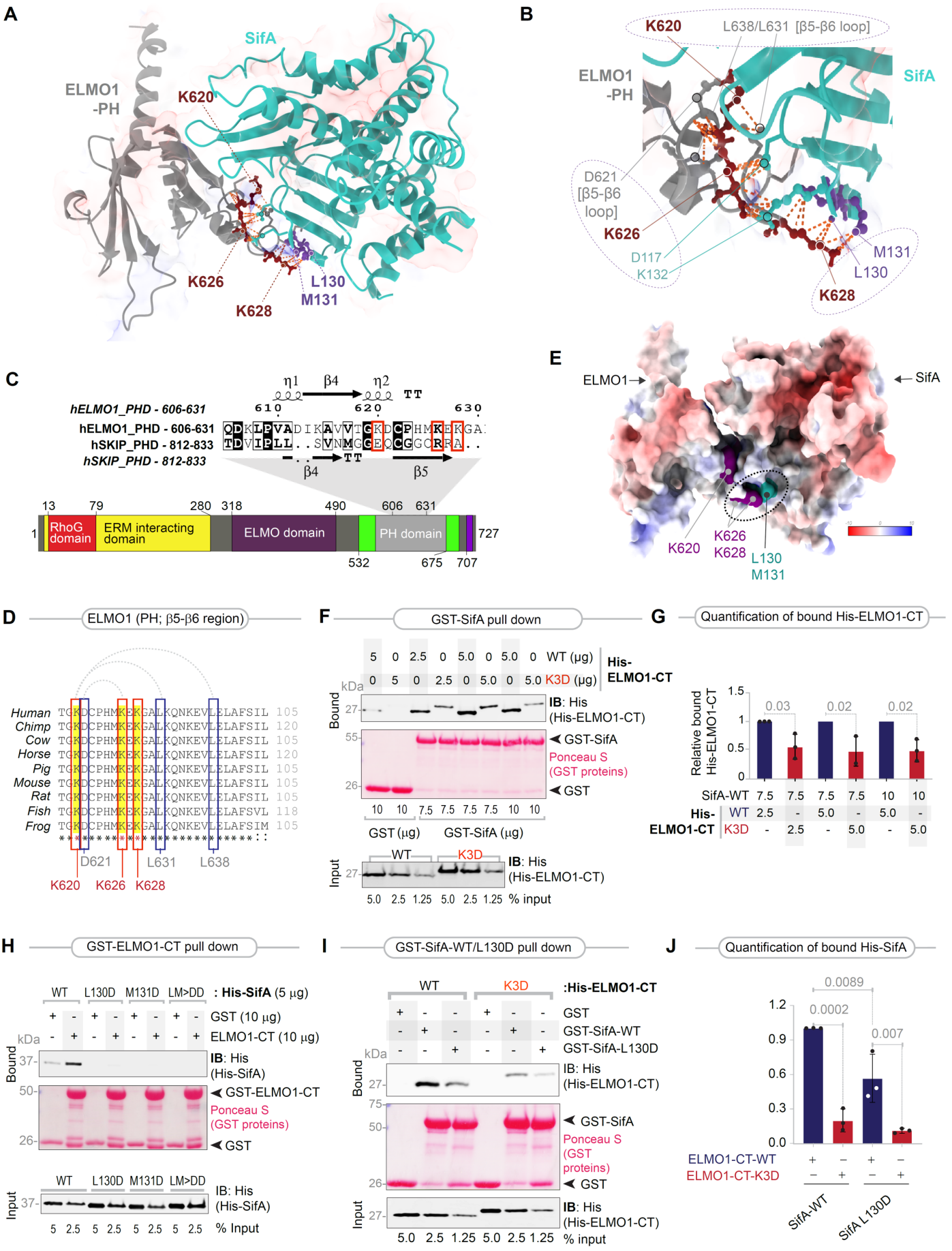

Figure 2: Characterization of the ELMO1•SifA interface.

A. Homology model of the ELMO1(gray)•SifA(turquoise) complex, generated by superimposing the solved structure of the ELMO1-PH (PDB:2VSZ) on that of the SKIP-PH in complex with SifA (PDB:3CXB). The executive root mean square deviation (RMSD) of the model is 1.528 (see **Fig. S1** for the workflow used to generate the homology models and select the fittest model with the most optimal parameters). The model is annotated with key amino acids that are predicted to form the interface. On ELMO1, these amino acids were identified as an evolutionarily conserved polar hotspot of three lysines within the β5-β6 loop, and their key intra- and intermolecular contacts on SifA are annotated. See **Supplemental Information 1** for a complete catalog of the inter- and intramolecular contacts of the highlighted residues. The distance between the residues calculated for contacts were within 4.0 A. See **Fig. S2** for the position of the WxxxE motif relative to the ELMO1•SifA interface.

B. A magnified view of the key residues participating at the ELMO1 (gray)•SifA (turquoise) interface. Three major clusters of inter- and intramolecular interactions of the lysine triad are annotated with interrupted circles/ovals. Lys(K)628 on (ELMO1) primarily engages via strong polar contacts with Met(M)131 and Leu(L)130 on SifA. K626 on (ELMO1) makes an intramolecular contact with D621, a residue within the β5-β6 loop; it is also juxtaposed with K132 and forms a 'charge-neutralizing' salt bridge with Asp(D)117 on SifA. K620 on (ELMO1) appears to primarily bind L631 and L638, which are key residue within the β5-β6 loop.

C. *Top*: An alignment of the sequences of the PH domains of ELMO1 and SKIP is shown, along with secondary structures. Conserved residues are shaded in black; similar residues are boxed. Three lysine residues on ELMO1 that correspond to the structurally resolved contact sites of SKIP for SifA are marked with red boxes. See also **Fig. S3A** for an extended alignment. *Bottom*: A domain map of ELMO1.

D. An alignment of the β5-β6 loop of ELMO1 showing that the lysine triad highlighted with red box in C is conserved across diverse species. Intra-loop interactions are indicated with interrupted arcs on top. Leu(L) and Asp(D) residues which are engaged in these interactions are also conserved and are highlighted with blue boxes. See also **Fig. S4** for extended alignment.

E. Panel displays APBS (Adaptive Poisson-Boltzmann Solver)-derived surface electrostatics for an all-side chain model of the ELMO1•SifA co-complex, as visualized using Chimaera. Volume surface coloring was set in the default range of -10 (red), through 0 (white), to +10 (blue) kT/e, where negatively charged surfaces are red (-10 kT/e) and positively charged surfaces are blue (+10 kT/e). In the most energetically favorable orientation, charged residues Lys(K)628 and Lys(K)626 on (ELMO1) bring hydrophobic residues Met(M)131 and Leu(L)130 on SifA into proximity [marked by an oval]. See **Fig. S5** for additional views.

F. Recombinant WT or K3D mutant His-ELMO1-CT proteins (~2.5 or 5 µg; Input) were used in pulldown assays with immobilized GST alone or GST-SifA (~7.5 or 10 µg). Bound ELMO1 was visualized by immunoblotting using an anti-His (ELMO1) antibody. GST proteins are visualized by Ponceau S staining. The K3D mutant, displayed slower electrophoretic mobility compared to the WT ELMO1 protein consistently in both reducing and non-reducing gels, and regardless of whether it was expressed in bacteria as

recombinant proteins or expressed in mammalian cells, suggesting it is likely to be due to the introduction of negative charge in the form of 3 aspartates.

G. Quantification of immunoblots in F. Results are displayed as mean ± S.D (n = 3 independent replicates). Statistical significance was determined using an unpaired t-test.

H. Equal aliquots (5 µg; Input) of recombinant His-SifA and its mutants (L130D, M131D, and LM-DD) were used in pulldown assays with immobilized GST alone or GST-ELMO1-CT (10 µg). Bound SifA proteins were visualized by immunoblotting using an anti-His antibody. GST proteins are visualized by Ponceau S staining.

I. Recombinant WT or K3D mutant His-ELMO1-CT proteins were used in pulldown assays with GST or GST-SifA (WT or L130D mutant). Bound ELMO1 was visualized by immunoblotting using an anti-His antibody. GST proteins are visualized by Ponceau S staining.

J. Quantification of immunoblots in I. Results are displayed as mean ± S.D (n = 3 independent replicates). Statistical significance was determined using an unpaired t-test.

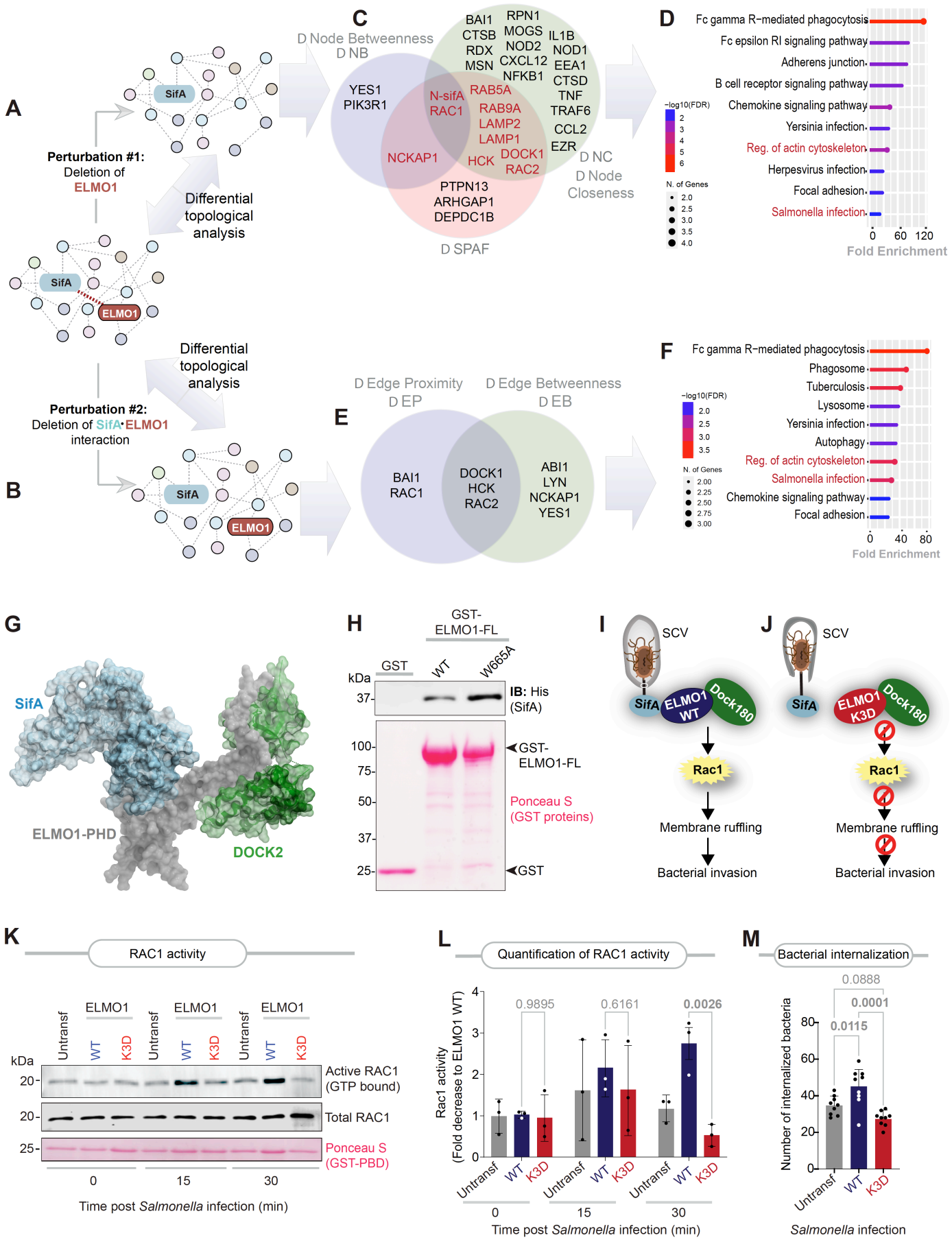

Figure 3. Prediction and validation of the consequences of disruption of the ELMO1•SifA interface.

A-B. A SifA (*Salmonella*)•human PPI network was constructed using a previously identified BioID-determined interactome of SifA (41) and their connectors were fetched from the human STRING database (54). Network perturbation was carried out *in-silico* either by deletion of ELMO1 (A; node deletion) or selective disruption of the ELMO1•SifA interaction (B; edge deletion).

C-D. Venn-diagram (C) shows sets of proteins that were impacted by *in-silico* deletion of ELMO1, as determined by three independent metrics of network topological analyses: differential node betweenness (ΔNB), node closeness (ΔNB) and shortest path alteration fraction (ΔSPAF). Lollipop plots (D) indicate the KEGG pathways enriched among the proteins that were identified as impacted based on more than one node-based metric. See **Fig. S6** for a detailed analysis.

E-F. Venn-diagram (E) shows sets of proteins that were impacted by *in-silico* deletion of the ELMO1•SifA interaction, as determined by two metrics of network topological analyses: differential edge betweenness (ΔEB) and edge proximity (ΔEP). Lollipop plots (F) indicate the KEGG pathways enriched among the proteins that were identified using edge-based metrices. See **Supplemental Information 2** for a detailed list of nodes and edges.

G. A homology model of a co-complex between SifA (light blue), ELMO1 (gray), and DOCK180 (green), built by overlaying resolved crystal structures of DOCK2•ELMO1 (PDB:3A98)(24), ELMO1 (PDB:2VSZ) and SifA•SKIP (PDB:3CXB).

H. Recombinant His-SifA (~5ug) were used in a GST pulldown assay with GST (negative control), and GST-tagged wild-type (WT) and W665A mutants of full length (FL) ELMO1, and bound SifA was visualized by immunoblot using anti-His (SifA) antibody. Equal loading of GST proteins is confirmed by Ponceau S staining.

I-J: Key steps in SifA•ELMO1•Dock180 co-complex mediated Rac1 signaling (I) and the predicted impact of selectively disrupting SifA•ELMO1 interaction using the K3D mutant (J) are shown.

K-L. ELMO1-depleted J774 macrophages (Untransfected) transfected with either WT or K3D mutant ELMO1 and subsequently infected with *Salmonella* (MOI 10; at indicated time points post-infection) were assessed for Rac1 activation by pulldown assays using GST-PBD. Immunoblots and Ponceau S-stained GST proteins are shown in K. Quantification of immunoblots in L. Results are displayed as mean ± S.D (n = 3 independent replicates). Statistical significance was determined using one-way ANOVA.

M: Bar graph represents the number of internalized bacteria by the same cells in K infected with *Salmonella* (MOI 10; 30 min post-infection). Results are displayed as mean ± S.D (n = 3 independent replicates). Statistical significance was determined using one-way ANOVA.

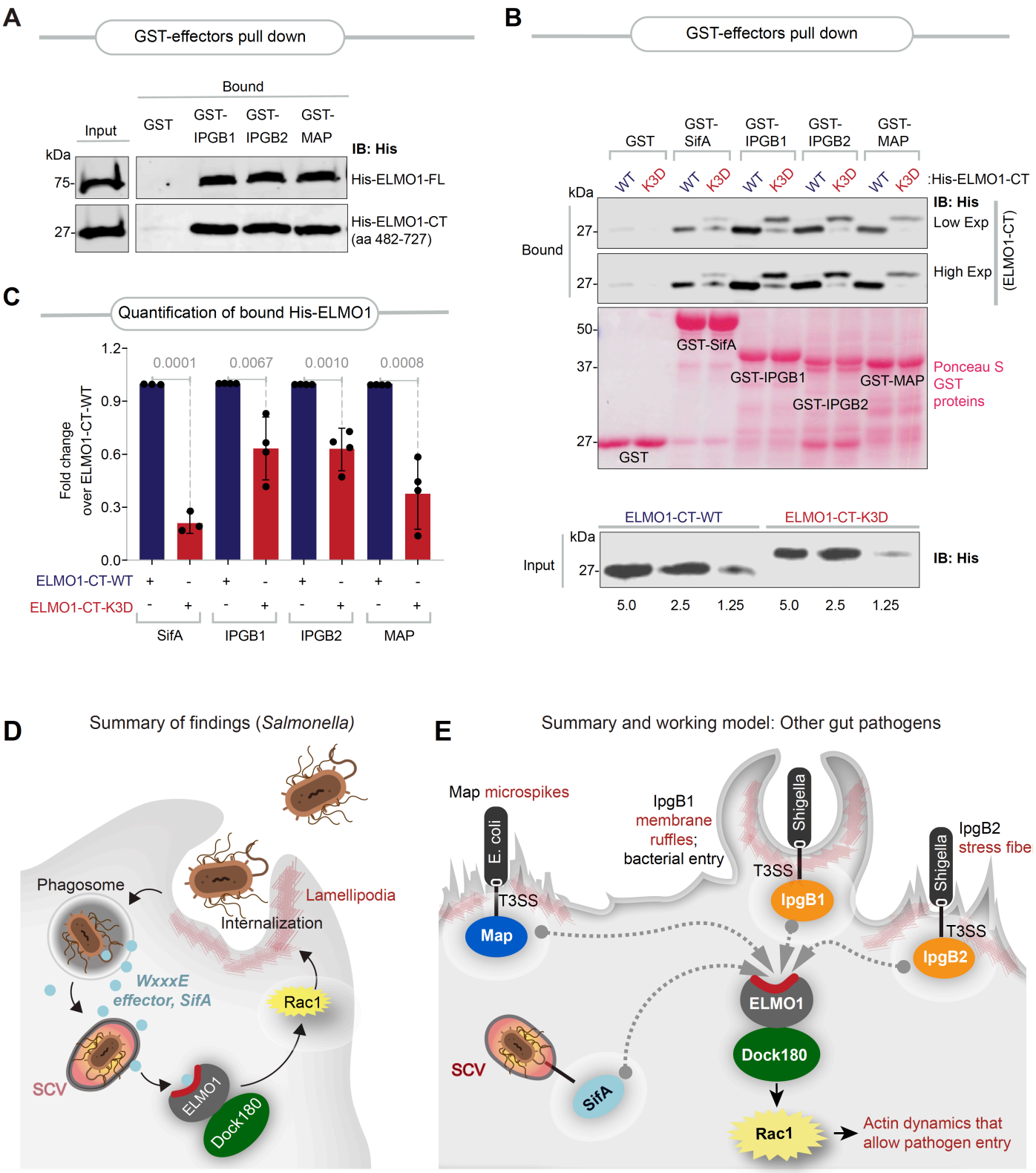

Figure 4: The SifA•ELMO1 interface is a conserved site for engaging diverse WxxxE-effectors.

A. Recombinant His-tagged CT (aa 482-727) or full-length (FL) ELMO1 proteins (~3 µg) were used in a pulldown assay with immobilized full-length GST-tagged WxxxE effectors (SifA, IpgB1, IpgB2, Map) or GST alone (negative control). Bound ELMO1 proteins were visualized by immunoblot using anti-His (SifA) antibody. GST proteins are visualized by Ponceau S staining.

B. Recombinant WT or K3D mutant His-ELMO1-CT proteins (~3 µg) were used in pulldown assays with immobilized GST-tagged full-length effectors as in A. Bound ELMO1 was visualized by immunoblotting using an anti-His antibody. GST proteins are visualized by Ponceau S staining.

C. Quantification of immunoblots in B. Results are displayed as mean ± S.D (n = 3 independent replicates). Statistical significance was determined using an unpaired t-test.

D-E. Schematic (D) summarizes the key findings in this work using *Salmonella* and its WxxxE-motif effector, SifA. Schematic (E) summarizes the key biochemical findings and the working model proposed for how diverse microbes use their *WxxxE* motif-containing virulence factors (effectors) to hijack the host engulfment pathway via a shared mechanism. Although diverse in sequence (see **Fig. S7** for an alignment of WxxxE effectors) and function, they all bind a conserved surface on ELMO1 (highlighted in red). The major consequence of such WxxxE-effector•ELMO1 interaction is enhanced Rac1 activation and bacterial engulfment.

EXPERIMENTAL PROCEDURES

Full experimental procedures can be found in the supporting information.

RESOURCE AVAILABILITY

LEAD CONTACT

Further information and requests for resources and reagents should be directed to and will be fulfilled by the lead contact, Pradipta Ghosh, prghosh@ucsd.edu.

MATERIALS AVAILABILITY

This study has generated constructs and cell lines. These materials can only be accessed through proper material transfer agreement following the guidelines of the University of California, San Diego.

DATA AND CODE AVAILABILITY

All data is available in the main text or the supplementary materials. Original western blot images and microscopy data will be shared by the lead contact upon request. This paper also analyzes an existing, publicly available proteomics dataset and protein structures (listed in the Key Resources Table). Source data for gene ontology analyses are provided with this paper. This paper includes PPI network analysis; a link to the codes is provided (**Key Resources Table**). Any additional information required to reanalyze the data reported in this paper is available from the lead contact upon request.

CATALOG OF SUPPLORTING MATERIALS

This article contains supporting information that includes.

1. Experimental procedures
2. Supplementary Figures and Legends (7)
3. Supplemental Information (2 Excel Datasheets; uploaded separately)

ACKNOWLEDGEMENTS

We thank Soumita Das (UC San Diego, CA; currently at University of Massachusetts, Lowell, MA) for numerous reagents and constructs that were used in this work and for helpful discussions. This work was supported by the National Institute of Health (NIH) Grants: R01-AI141630, UG3TR003355, UG3TR002968 and R01-AI55696 (P.G). PG was also supported by the Leona M. and Harry B. Helmsley Charitable Trust and NIH programs. G.D.K. was supported through The American Association of Immunologists (AAI) Intersect Fellowship Program for Computational Scientists and Immunologists. S.R was supported, in part, by the NIH grants (AI118985 and GM117424) and M.A was supported by R01-DK107585 and R01-AI141630. S.R.I was supported by a NIH Diversity Supplement award (3R01DK107585-02S1). We thank Ying Jones (UC San Diego Electron Microscopy Core Facility) for technical and logistical support. The content is solely the responsibility of the authors and does not necessarily represent the official views of the Helmsley Charitable Trust or the National Institutes of Health.

AUTHOR CONTRIBUTIONS

M. A., and P.G. designed, executed, and analyzed most of the experiments and/or formal analysis in this work. M.A carried out all the biochemical and functional assays. M.A. and G.K. carried out semi-quantitative transmission-electron microscopy (TEM). S. R, with assistance from A.B, generated and analyzed the sequence and structure homology models and carried out APBS analyses. S. S. created and analyzed the PPI networks. S.R.C. generated the mutant constructs. H.G. and A.A. provided technical assistance for bacterial clearance studies. G.K. and P.G. prepared and/or created display items for data visualization and/or presentation. M.A, G.K. and P.G wrote the manuscript. All authors reviewed and edited the manuscript and approved its final version.

CONFLICT OF INTERESTS

The authors declare no competing interests.

REFERENCES

1. Steele-Mortimer, O. (2008) The Salmonella-containing vacuole: moving with the times Curr Opin Microbiol **11**, 38-45 10.1016/j.mib.2008.01.002
2. Castanheira, S., andGarcía-Del Portillo, F. (2017) Salmonella Populations inside Host Cells Front Cell Infect Microbiol **7**, 432 10.3389/fcimb.2017.00432
3. Lai, Y., Rosenshine, I., Leong, J. M., andFrankel, G. (2013) Intimate host attachment: enteropathogenic and enterohaemorrhagic Escherichia coli Cell Microbiol **15**, 1796-1808 10.1111/cmi.12179
4. Smith, K., Humphreys, D., Hume, P. J., andKoronakis, V. (2010) Enteropathogenic Escherichia coli recruits the cellular inositol phosphatase SHIP2 to regulate actin-pedestal formation Cell Host Microbe **7**, 13-24 10.1016/j.chom.2009.12.004
5. Watson, J. L., Sanchez-Garrido, J., Goddard, P. J., Torraca, V., Mostowy, S., Shenoy, A. R. *et al.* (2019) Shigella sonnei O-Antigen Inhibits Internalization, Vacuole Escape, and Inflammasome Activation mBio **10**, 10.1128/mBio.02654-19
6. Handa, Y., Suzuki, M., Ohya, K., Iwai, H., Ishijima, N., Koleske, A. J. *et al.* (2007) Shigella IpgB1 promotes bacterial entry through the ELMO-Dock180 machinery Nat Cell Biol **9**, 121-128 10.1038/ncb1526
7. Finlay, B. B., andCossart, P. (1997) Exploitation of mammalian host cell functions by bacterial pathogens Science **276**, 718-725 10.1126/science.276.5313.718
8. Galán, J. E., andCollmer, A. (1999) Type III secretion machines: bacterial devices for protein delivery into host cells Science **284**, 1322-1328 10.1126/science.284.5418.1322
9. Cossart, P., andSansonetti, P. J. (2004) Bacterial invasion: the paradigms of enteroinvasive pathogens Science **304**, 242-248 10.1126/science.1090124
10. Connor, M. G., Pulsifer, A. R., Chung, D., Rouchka, E. C., Ceresa, B. K., andLawrenz, M. B. (2018) Yersinia pestis Targets the Host Endosome Recycling Pathway during the Biogenesis of the Yersinia-Containing Vacuole To Avoid Killing by Macrophages mBio **9**, 10.1128/mBio.01800-17
11. Watson, R. O., andGalán, J. E. (2008) Campylobacter jejuni survives within epithelial cells by avoiding delivery to lysosomes PLoS Pathog **4**, e14 10.1371/journal.ppat.0040014
12. Coburn, B., Sekirov, I., andFinlay, B. B. (2007) Type III secretion systems and disease Clin Microbiol Rev **20**, 535-549 10.1128/cmr.00013-07
13. Orchard, R. C., Kittisopikul, M., Altschuler, S. J., Wu, L. F., Süel, G. M., andAlto, N. M. (2012) Identification of F-actin as the dynamic hub in a microbial-induced GTPase polarity circuit Cell **148**, 803-815 10.1016/j.cell.2011.11.063
14. Alto, N. M., Shao, F., Lazar, C. S., Brost, R. L., Chua, G., Mattoo, S. *et al.* (2006) Identification of a bacterial type III effector family with G protein mimicry functions Cell **124**, 133-145 10.1016/j.cell.2005.10.031
15. Bulgin, R., Raymond, B., Garnett, J. A., Frankel, G., Crepin, V. F., Berger, C. N. *et al.* (2010) Bacterial guanine nucleotide exchange factors SopE-like and WxxxE effectors Infect Immun **78**, 1417-1425 10.1128/iai.01250-09
16. Hardt, W. D., Chen, L. M., Schuebel, K. E., Bustelo, X. R., andGalán, J. E. (1998) S. typhimurium encodes an activator of Rho GTPases that induces membrane ruffling and nuclear responses in host cells Cell **93**, 815-826 10.1016/s0092-8674(00)81442-7
17. Ohya, K., Handa, Y., Ogawa, M., Suzuki, M., andSasakawa, C. (2005) IpgB1 is a novel Shigella effector protein involved in bacterial invasion of host cells. Its activity to promote membrane ruffling via Rac1 and Cdc42 activation J Biol Chem **280**, 24022-24034 10.1074/jbc.M502509200
18. Bulgin, R. R., Arbeloa, A., Chung, J. C., andFrankel, G. (2009) EspT triggers formation of lamellipodia and membrane ruffles through activation of Rac-1 and Cdc42 Cell Microbiol **11**, 217-229 10.1111/j.1462-5822.2008.01248.x
19. Arbeloa, A., Bulgin, R. R., MacKenzie, G., Shaw, R. K., Pallen, M. J., Crepin, V. F. *et al.* (2008) Subversion of actin dynamics by EspM effectors of attaching and effacing bacterial pathogens Cell Microbiol **10**, 1429-1441 10.1111/j.1462-5822.2008.01136.x
20. Kenny, B., Ellis, S., Leard, A. D., Warawa, J., Mellor, H., andJepson, M. A. (2002) Co-ordinate regulation of distinct host cell signalling pathways by multifunctional enteropathogenic Escherichia coli effector molecules Mol Microbiol **44**, 1095-1107 10.1046/j.1365-2958.2002.02952.x
21. Sayed, I. M., Ibeawuchi, S. R., Lie, D., Anandachar, M. S., Pranadinata, R., Raffatellu, M. *et al.* (2021) The interaction of enteric bacterial effectors with the host engulfment pathway control innate immune responses Gut Microbes **13**, 1991776 10.1080/19490976.2021.1991776

22. Xue, R., Wang, Y., Wang, T., Lyu, M., Mo, G., Fan, X. *et al.* (2021) Functional Verification of Novel ELMO1 Variants by Live Imaging in Zebrafish Front Cell Dev Biol **9**, 723804 10.3389/fcell.2021.723804
23. Grimsley, C. M., Kinchen, J. M., Tosello-Trampont, A. C., Brugnera, E., Haney, L. B., Lu, M. *et al.* (2004) Dock180 and ELMO1 proteins cooperate to promote evolutionarily conserved Rac-dependent cell migration J Biol Chem **279**, 6087-6097 10.1074/jbc.M307087200
24. Hanawa-Suetsugu, K., Kukimoto-Niino, M., Mishima-Tsumagari, C., Akasaka, R., Ohsawa, N., Sekine, S. *et al.* (2012) Structural basis for mutual relief of the Rac guanine nucleotide exchange factor DOCK2 and its partner ELMO1 from their autoinhibited forms Proc Natl Acad Sci U S A **109**, 3305-3310 10.1073/pnas.1113512109
25. Kukimoto-Niino, M., Ihara, K., Murayama, K., andShirouzu, M. (2021) Structural insights into the small GTPase specificity of the DOCK guanine nucleotide exchange factors Curr Opin Struct Biol **71**, 249-258 10.1016/j.sbi.2021.08.001
26. Diacovich, L., Dumont, A., Lafitte, D., Soprano, E., Guilhon, A. A., Bignon, C. *et al.* (2009) Interaction between the SifA virulence factor and its host target SKIP is essential for Salmonella pathogenesis J Biol Chem **284**, 33151-33160 10.1074/jbc.M109.034975
27. Lin, Q., Yang, W., Baird, D., Feng, Q., andCerione, R. A. (2006) Identification of a DOCK180-related guanine nucleotide exchange factor that is capable of mediating a positive feedback activation of Cdc42 J Biol Chem **281**, 35253-35262 10.1074/jbc.M606248200
28. Toret, C. P., Collins, C., andNelson, W. J. (2014) An Elmo-Dock complex locally controls Rho GTPases and actin remodeling during cadherin-mediated adhesion J Cell Biol **207**, 577-587 10.1083/jcb.201406135
29. Achi, S. C., Karimilangi, S., Lie, D., Sayed, I. M., andDas, S. (2023) The WxxxE proteins in microbial pathogenesis Crit Rev Microbiol **49**, 197-213 10.1080/1040841x.2022.2046546
30. Huang, Z., Sutton, S. E., Wallenfang, A. J., Orchard, R. C., Wu, X., Feng, Y. *et al.* (2009) Structural insights into host GTPase isoform selection by a family of bacterial GEF mimics Nat Struct Mol Biol **16**, 853-860 10.1038/nsmb.1647
31. Klink, B. U., Barden, S., Heidler, T. V., Borchers, C., Ladwein, M., Stradal, T. E. *et al.* (2010) Structure of Shigella IpgB2 in complex with human RhoA: implications for the mechanism of bacterial guanine nucleotide exchange factor mimicry J Biol Chem **285**, 17197-17208 10.1074/jbc.M110.107953
32. Ohlson, M. B., Huang, Z., Alto, N. M., Blanc, M. P., Dixon, J. E., Chai, J. *et al.* (2008) Structure and function of Salmonella SifA indicate that its interactions with SKIP, SseJ, and RhoA family GTPases induce endosomal tubulation Cell Host Microbe **4**, 434-446 10.1016/j.chom.2008.08.012
33. Arbeloa, A., Garnett, J., Lillington, J., Bulgin, R. R., Berger, C. N., Lea, S. M. *et al.* (2010) EspM2 is a RhoA guanine nucleotide exchange factor Cell Microbiol **12**, 654-664 10.1111/j.1462-5822.2009.01423.x
34. Raymond, B., Crepin, V. F., Collins, J. W., andFrankel, G. (2011) The WxxxE effector EspT triggers expression of immune mediators in an Erk/JNK and NF-κB-dependent manner Cell Microbiol **13**, 1881-1893 10.1111/j.1462-5822.2011.01666.x
35. Das, S., Sarkar, A., Choudhury, S. S., Owen, K. A., Castillo, V., Fox, S. *et al.* (2015) ELMO1 has an essential role in the internalization of Salmonella Typhimurium into enteric macrophages that impacts disease outcome Cell Mol Gastroenterol Hepatol **1**, 311-324 10.1016/j.jcmgh.2015.02.003
36. Ruiz-Albert, J., Yu, X. J., Beuzón, C. R., Blakey, A. N., Galyov, E. E., andHolden, D. W. (2002) Complementary activities of SseJ and SifA regulate dynamics of the Salmonella typhimurium vacuolar membrane Mol Microbiol **44**, 645-661 10.1046/j.1365-2958.2002.02912.x
37. Beuzón, C. R., Méresse, S., Unsworth, K. E., Ruíz-Albert, J., Garvis, S., Waterman, S. R. *et al.* (2000) Salmonella maintains the integrity of its intracellular vacuole through the action of SifA Embo j **19**, 3235-3249 10.1093/emboj/19.13.3235
38. Arpaia, N., Godec, J., Lau, L., Sivick, K. E., McLaughlin, L. M., Jones, M. B. *et al.* (2011) TLR signaling is required for Salmonella typhimurium virulence Cell **144**, 675-688 10.1016/j.cell.2011.01.031
39. Dumont, A., Boucrot, E., Drevensek, S., Daire, V., Gorvel, J. P., Poüs, C. *et al.* (2010) SKIP, the host target of the Salmonella virulence factor SifA, promotes kinesin-1-dependent vacuolar membrane exchanges Traffic **11**, 899-911 10.1111/j.1600-0854.2010.01069.x
40. Jurrus, E., Engel, D., Star, K., Monson, K., Brandi, J., Felberg, L. E. *et al.* (2018) Improvements to the APBS biomolecular solvation software suite Protein Sci **27**, 112-128 10.1002/pro.3280
41. D'Costa, V. M., Coyaud, E., Boddy, K. C., Laurent, E. M. N., St-Germain, J., Li, T. *et al.* (2019) BioID screen of Salmonella type 3 secreted effectors reveals host factors involved in vacuole positioning and stability during infection Nat Microbiol **4**, 2511-2522 10.1038/s41564-019-0580-9

42. Sarkar, A., Tindle, C., Pranadinata, R. F., Reed, S., Eckmann, L., Stappenbeck, T. S. *et al.* (2017) ELMO1 Regulates Autophagy Induction and Bacterial Clearance During Enteric Infection J Infect Dis **216**, 1655-1666 10.1093/infdis/jix528
43. Sayed, I. M., Suarez, K., Lim, E., Singh, S., Pereira, M., Ibeawuchi, S. R. *et al.* (2020) Host engulfment pathway controls inflammation in inflammatory bowel disease Febs j **287**, 3967-3988 10.1111/febs.15236
44. Makino, Y., Tsuda, M., Ohba, Y., Nishihara, H., Sawa, H., Nagashima, K. *et al.* (2015) Tyr724 phosphorylation of ELMO1 by Src is involved in cell spreading and migration via Rac1 activation Cell Commun Signal **13**, 35 10.1186/s12964-015-0113-y
45. Yokoyama, N., deBakker, C. D., Zappacosta, F., Huddleston, M. J., Annan, R. S., Ravichandran, K. S. *et al.* (2005) Identification of tyrosine residues on ELMO1 that are phosphorylated by the Src-family kinase Hck Biochemistry **44**, 8841-8849 10.1021/bi0500832
46. Kukimoto-Niino, M., Katsura, K., Kaushik, R., Ehara, H., Yokoyama, T., Uchikubo-Kamo, T. *et al.* (2021) Cryo-EM structure of the human ELMO1-DOCK5-Rac1 complex Sci Adv **7**, 10.1126/sciadv.abg3147
47. Lu, M., Kinchen, J. M., Rossman, K. L., Grimsley, C., deBakker, C., Brugnera, E. *et al.* (2004) PH domain of ELMO functions in trans to regulate Rac activation via Dock180 Nat Struct Mol Biol **11**, 756-762 10.1038/nsmb800
48. Jackson, L. K., Nawabi, P., Hentea, C., Roark, E. A., andHaldar, K. (2008) The Salmonella virulence protein SifA is a G protein antagonist Proc Natl Acad Sci U S A **105**, 14141-14146 10.1073/pnas.0801872105
49. Li, Y., Huang, Y., Swaminathan, C. P., Smith-Gill, S. J., andMariuzza, R. A. (2005) Magnitude of the hydrophobic effect at central versus peripheral sites in protein-protein interfaces Structure **13**, 297-307 10.1016/j.str.2004.12.012
50. Ambler, R. P., andRees, M. W. (1959) Epsilon-N-Methyl-lysine in bacterial flagellar protein Nature **184**, 56-57 10.1038/184056b0
51. Huang, J., Sengupta, R., Espejo, A. B., Lee, M. G., Dorsey, J. A., Richter, M. *et al.* (2007) p53 is regulated by the lysine demethylase LSD1 Nature **449**, 105-108 10.1038/nature06092
52. Makino, Y., Tsuda, M., Ichihara, S., Watanabe, T., Sakai, M., Sawa, H. *et al.* (2006) Elmo1 inhibits ubiquitylation of Dock180 J Cell Sci **119**, 923-932 10.1242/jcs.02797
53. Song, J. H., Mascarenhas, J. B., Sammani, S., Kempf, C. L., Cai, H., Camp, S. M. *et al.* (2022) TLR4 activation induces inflammatory vascular permeability via Dock1 targeting and NOX4 upregulation Biochim Biophys Acta Mol Basis Dis **1868**, 166562 10.1016/j.bbadis.2022.166562
54. Szklarczyk, D., Gable, A. L., Nastou, K. C., Lyon, D., Kirsch, R., Pyysalo, S. *et al.* (2021) The STRING database in 2021: customizable protein-protein networks, and functional characterization of user-uploaded gene/measurement sets Nucleic Acids Res **49**, D605-D612 10.1093/nar/gkaa1074

Supporting information

Diverse gut pathogens exploit the host engulfment pathway via a conserved mechanism

AUTHORS:
Mahitha Shree Anandachar[1,2], Suchismita Roy[1], Saptarshi Sinha[1], Agyekum Boadi[1], Stella-Rita Ibeawuchi[2], Hobie Gementera[2], Alicia Amamoto[2], Gajanan D. Katkar[1]* and Pradipta Ghosh[1, 3]*

AFFILIATIONS:
[1]*Department of Cellular and Molecular Medicine, University of California San Diego.*
[2]*Department of Pathology, University of California San Diego.*
[3]*Department of Medicine, University of California San Diego.*

RUNNING TITLE: Gut pathogens exploit host's engulfment pathway

***CORRESPONDING AUTHORS:**

Gajanan D. Katkar, Ph.D.; Departments of Cellular and Molecular Medicine, University of California San Diego, CA 92093. **Phone**: 858-346-3507: **Email:** kgajanandattatray@ucsd.edu

Pradipta Ghosh, M.D.; Professor, Departments of Medicine and Cellular and Molecular Medicine, University of California San Diego, CA 92093. **Phone**: 858-822-7633: **Email:** prghosh@ucsd.edu

CATALOG OF SUPPORTING MATERIALS

1. *Key Resources and Detailed Experimental procedures*
2. *Supplementary Figures and Legends (7)*
3. *Supplemental Information (2 Excel Datasheets; uploaded separately)*

Experimental procedures

TABLE OF KEY RESOURCES

REAGENT or RESOURCE	SOURCE	IDENTIFIER
Antibodies		
Mouse monoclonal anti-poly-His	Sigma-Aldrich	Cat# H1029
Mouse monoclonal anti-FLAG	Cell Signaling	Cat# 8146S
Mouse monoclonal ELMO1 antibody	Santa Cruz Biotechnology	Cat# sc-271519
IRDye 800CW Goat anti-Mouse IgG Secondary	LI-COR Biosciences	Cat# 926-32210
IRDye 680RD Goat anti-Rabbit IgG Secondary	LI-COR Biosciences	Cat# 926-68071
Biological samples		
HEK 293	ATCC	CRL-1573
sh Control J774 and sh ELMO1 J774 murine macrophage cell lines	Sayed et al., 2021(1)	n/a
Salmonella enteric serovar Typhimurium (strain SL1344)	ATCC	Cat#700720
SifA mutant strain	Obtained from Olivia Steele-Mortimer (NIH/NIAID)	n/a
Chemicals, peptides		
HisPur™ Cobalt Resin	Thermo Scientific	Cat# 89964
Glutathione Sepharose® 4B	Sigma-Aldrich	Cat# GE17-0756-04
PVDF Transfer Membrane, 0.45mM	Thermo Scientific	Cat# 88518
Polyethylenimine (PEI)	Polysciences	Cat# Inc 23966
Protease inhibitor cocktail	Roche	Cat# 11 873 580 001
Critical commercial assay kits		
Rac1 Pull-Down Activation Assay Biochem Kit (Bead Pull-Down Format)	Cytoskeleton.Inc.	Cat# BK035-S
Plasmids and recombinant proteins		
pGEX-6P-2 (GST)	GE Healthcare	Cat# 28-9546-50
GST ELMO1 full-length (FL)	Sayed et al., 2021(1)	n/a
GST ELMO1 CT (aa 482-727)	*This paper*	n/a
GST SifA WT	Sayed et al., 2021(1)	n/a
GST SifA L130D	*This paper*	n/a
GST-IPGB1	*This paper*	Cloned from FLAG-IPGB1 provided by Neil Alto, UT Dallas
GST-IPGB2	*This paper*	Cloned from FLAG-IPGB2 provided by Neil Alto, UT Dallas
GST- MAP	*This paper*	Cloned from FLAG-Map provided by Neil Alto, UT Dallas
pET-28a (His)	Novagene	Cat# 69864
His ELMO1 full-length (FL)	*This paper*	n/a
His ELMO1 CT (aa 482-727)	*This paper*	n/a
His ELMO1 K620D/K626D/K628D	*This paper*	n/a
His SifA WT	*This paper*	n/a
His SifA L130D	*This paper*	n/a

His SifA M131D	*This paper*	n/a
His SifA L130D/M131D	*This paper*	n/a
FLAG ELMO1 (WT)	Sayed et al., 2021(1)	n/a
FLAG ELMO1 (K3D)	*This paper*	K620D; K626D; K628D
Mutagenesis Primers	**Forward primer**	**Reverse primer**
Mouse ELMO1 K620D/K626D/K628D	5'-tgttttgtttaagggcaccatcctcatccatatgaggcagtcctttcccgtc-3' 5'-gacgggaaaggactgccctcatatggatgaggatggtgcccttaaacaaaaca-3' 5'-caaagcagtggtgacgggagatgactgccctcatatgaaag-3'	5'-ctttcatatgagggcagtcatctcccgtcaccactgctttg-3'
SifA L130D	5'-ccgggcgatctttcatatcaaaataaagattccccatgacttcacagct-3'	5'-agctgtgaagtcatggggaatctttattttgatatgaaagatcgcccgg-3'
SifA M131D	5'-ttaaaatatccgggcgatctttatcatcaaaataaagattccccatgacttcacagc-3'	5'-gctgtgaagtcatggggaatctttattttgatgataaagatcgcccggatattttaa-3'
Cloning Primers	**Forward primer (5'→3')**	**Reverse primer (5'→3')**
Elmo1FL		
Elmo1 CT (BamHI/Not1)	cgcggatccatgcaggtggtgaaggagcagg	gcgacgcggccgctgttacagtcatagacaaagtcatagttgctaggttcct
IPGB1 (KpnI/BamHI)	catggtaccatgcaaattctaaacaaaatacttccacaggt	cgcggatccttaatttgtattgctttgacggtatacagcctt
IPGB2 (KpnI/BamHI)	catggtaccatgcttggaacatcttttaataattttggaatcagt	cgcggatcctcagaaaggcgattctaaatttgtaatatagtcac
MAP (EcoRI/KpnI)	ccggaattccatgtttagtccaatgacaatggcagg	catggtaccctacaatcgggtatcctgtacatgctc
Software and algorithms		
ImageStudio Lite	LI-COR	https://www.licor.com/bio/image-studio-lite/
Prism	GraphPad	Home - GraphPad
PyMOL Molecular Graphics System		https://pymol.org/2
ShinyGO v0.76		http://bioinformatics.sdstate.edu/go/
Codes for the construction and analysis of the PPI networks		https://github.com/sinha7290/ELMO
Publicly deposited structures and/or datasets		
ELMO1 (PH domain)	PDB:2VSZ	https://www.rcsb.org/structure/2VSZ
SKIP-PH bound to SifA	PDB:3CXB	https://www.rcsb.org/structure/3CXB
DOCK2-bound to ELMO1	PDB:3A98	https://www.rcsb.org/structure/3A98
Proximity ligation assay (BioID)	SifA interactome	D'Costa VM et al.,(2)

EXPERIMENTAL MODEL AND SUBJECT DETAILS

J774 macrophage and human (HEK) cell lines were used in various assays. Bacterial strains were used to infect macrophages in various experiments. This study does not involve the use of human subjects or animals.

METHOD DETAILS

Plasmid constructs and mutagenesis.

ELMO1 and SifA (from SL1344) were amplified by PCR and cloned into pET-28a (+) and pGEX-6P-2 plasmid vectors to generate His- and GST-tagged proteins, respectively. ELMO1 CT (aa 482-727) was amplified by PCR from human ELMO1 cDNA (Clone IRAUp969C0316D, SourceBioscience Inc) and subcloned into pET-28a (+) and pGEX-6P-2 plasmid vectors using BamHI and NotI restriction sites. Effector proteins IPGB1, IPGB2 and MAP were amplified from FLAG-tagged effector constructs (obtained from Neil Alto, UT Dallas) and cloned into pGEX-6P-2 plasmid vectors. ELMO1 and SifA mutations were generated by site directed mutagenesis using the Quick-Change II Site-Directed Mutagenesis kit (Agilent Technologies) and specific primers (**table of key resources**) according to manufacturer's protocol. All plasmid constructs and mutagenesis were verified by sequencing and protein expression was verified by western blot analysis.

Bacteria and bacterial culture

Salmonella enterica serovar *Typhimurium* strain SL1344, were obtained from the American Type Culture Collection (ATCC) (Manassas, VA, USA), and SL1344 Δ*SifA* mutant strain was obtained from Olivia Steele Mortimer (NIH/NIAID) (3, 4) . The bacterial strains were propagated as described previously (5, 6). Briefly, a single colony was inoculated into LB broth and grown for 8 h under aerobic conditions and then under oxygen-limiting conditions. For SL1344 Δ*SifA* mutant strain, streptomycin with final conc (100 µg/mL) was added to LB broth. Cells were infected with a multiplicity of infection (moi) of 10.

Cell culture and transfection

HEK cells were obtained from American Type Culture Collection, (Manassas, VA, USA). Control and ELMO1 depleted shRNA J774 cells were generated as previously described (7). Cells were maintained in high glucose DMEM (Life Technologies) containing 10% fetal bovine serum and 100 U/ml penicillin and streptomycin at 37°C in a 5% CO2 incubator. Cells were sub-cultured 24 h prior to transfection. Transfections of plasmids were performed using Lipofectamine 2000 (Invitrogen) according to manufacturer's protocol.

Transmission electron microscopy (TEM)

Control (shControl) and ELMO1-depleted (shELMO1) J477 macrophages were infected with *Salmonella* enterica serovar *Typhimurium* strain SL1344 (SL) and its mutant strain *SifA* [MOI 30] and the infected pellets were fixed with Glutaraldehyde in 0.1 M Sodium Cacodylate Buffer, (pH 7.4) followed by post-fixation with 1% OsO4 in 0.1 M cacodylate buffer for 1 h on ice followed by staining with 2% uranyl acetate for 1 h and dehydrated in ethanol

(50-100%) on ice. The cells were washed for 10 min each once with 100% ethanol and two times with acetone and embedded with Durcupan. A Leica UCT ultramicrotome was used to section 60 nm cuts and picked up on 300 mesh copper grids. Sections were post-stained first with 2% uranyl acetate (5 min) and Sato's lead stain (1 min) prior to visualization using a JEOL-1400plus equipped with a bottom-mount Gatan (4k x 4k) camera.

Protein expression and purification

Recombinant His and GST-tagged proteins were expressed in Escherichia coli strain BL21 (DE3) and purified as previously described (1, 2). Briefly, proteins in bacterial culture were induced with IPTG (1 mM) overnight incubation at 25°C. Centrifuged and cell pellet were then lysed in either GST lysis buffer containing 25 mM Tris-HCl (pH 7.4) 20 mM NaCl, 1 mM EDTA, 20% (v/v) glycerol, 1% (v/v) Triton X-100, protease inhibitor cocktail or His lysis buffer containing 50 mM NaH_2PO_4 (pH 7.4), 300 mM NaCl, 10 mM imidazole, 1% (v/v) Triton-X-100, protease inhibitor cocktail and then sonicated briefly to ensure better lysis. Cell lysate were centrifugation at 12,000 x g at 4°C for 30 mins to remove cell debris. Cleared cell lysate was then affinity purified using either glutathione-Sepharose 4B beads or HisPur Cobalt Resin, followed by elution and overnight dialysis in PBS. Proteins were aliquoted and stored at -80°C prior to use.

GST pulldown assays

Recombinant purified GST-tagged proteins were immobilized onto glutathione-Sepharose beads in a binding buffer containing 50 mM Tris-HCl (pH 7.4), 100 mM NaCl, 0.4% (v/v) Nonidet P-40, 10 mM $MgCl_2$, 5 mM EDTA, 2 mM DTT for 60 min at 4°C. GST-tagged protein bound beads were washed and incubated with purified His-tagged proteins in a binding buffer for 4 h at 4°C. Protein bound complexes on a beads were washed four times with phosphate wash buffer containing 4.3 mM Na_2HPO_4, 1.4 mM KH_2PO_4 (pH 7.4), 137 mM NaCl, 2.7 mM KCl, 0.1% (v/v) Tween-20, 10 mM $MgCl_2$, 5 mM EDTA, 2 mM DTT, 0.5 mM sodium orthovanadate and eluted by boiling beads in reducing sample buffer containing 5% SDS, 156 mM Tris-Base, 25% glycerol, 0.025% bromophenol blue, 25% β-mercaptoethanol. Bound proteins and lysates were fractionated by SDS/PAGE gel and analyzed by immunoblot.

Quantitative immunoblotting

For immunoblotting, protein samples were separated by 10% SDS-PAGE and transferred to polyvinylidene fluoride (PVDF) membranes. Membranes were blocked with 5% non-fat milk in Tris-buffered saline with 0.1% Tween® 20 detergent (1X TBST). The membrane was stained with Ponceau S to visualize bait proteins (GST), washed, blocked (5% milk), and incubated with primary antibody solutions overnight at 4°C (unless otherwise specified, a 1:500 dilution for primary antibody was used). Washed blots were then incubated with infrared secondary antibodies (see Key Resource Table) for 1 h at room temperature. Dual color infrared imaging and quantifications of immunoblots were performed using a Li-Cor Odyssey imaging system and analyzed using the Image StudioLite software as per manufacturer's instructions.

Homology modelling and protein docking

For the structure-guided mutagenesis studies, we took into consideration the following three previously resolved structures, all accessed through the Protein Data Bank (PDB; https://www.rcsb.org/)-- (i) PDB:3CXB, a 2.60 Å resolved crystal structure of the PH domain of SKIP (3CXB, golden brown) in complex with full length SifA (3CXB, cyan; (ii) PDB:2VSZ, a 2.30 Å resolved crystal structure of the C-terminal 200 aa (containing the PH domain) of ELMO1 in complex with the N-terminal 200 aa of DOCK180; (iii) PDB:3A98, a 2.10 N-terminal 177 aa fragment of DOCK2 and the C-terminal 196 aa fragment (containing the PH domain) of ELMO1. First, the PH domain of SKIP (PDB:3CXB; template) was superimposed to the PH-domain of ELMO1 (PDB:2VSZ). The performed analysis of the PH domains revealed them to be quite similar in structure SKIP and ELMO1 (RMSD of 1.528). Subsequently, the PH domain was used for molecular docking with SifA. Protein docking and the prediction of the contact sites at the ELMO1•SifA interface was performed by using HADDOCK (High Ambiguity Driven protein−protein Docking (8)) web server and the final representation was using Pymol visualization tool (https://pymol.org/2/; The PyMOL Molecular Graphics System. Delano Scientific, San Carlos). HADDOCK is a popular docking program that takes a data-driven approach to docking, with support for a wide range of experimental data (8). HADDOCK generated **130** structures in **15** cluster(s), which represents **65 %** of the water-refined models. The HADDOCK scoring function consists of a linear combination of various energies and buried surface area (HADDOCK2.2 scoring function). Based on such HADDOCK scoring, the models in cluster #3 were most optimal based on the Z-score which indicates how many standard deviations from the average this cluster is located in terms of score (the more negative the better). For cluster 3 we got a Z score of -1.5 and HADDOCK score of -59.7 (**Fig. S1**). The best fit co-complex model was used for predicting the properties and nature of the protein-protein binding interface. A complete list of contacts is provided in **Supplemental Information 1** as an excel datasheet. For calculating the electrostatic surface potential (kT/e) for the ELMO1•SifA co-complex we used adaptive Poisson-Boltzmann solver (APBS), an NIH-supported software (9)[https://www.poissonboltzmann.org/] for the analysis of electrostatic forces for large bimolecular assemblages. The APBS derived surface potential of the ELMO:SifA complex was visualized using Chimaera UCSF software (10). Amino acids were color-coded (red negatively charged; blue positively charged) based on the values of APBS scale in a range of -10 to +10 kT/e as default settings.

Construction, perturbation, and analysis of the Protein-Protein Interaction Network

A SifA (*Salmonella*)•human interaction network was constructed using a previously identified BioID-determined interactome of SifA (11) and their connectors, fetched from the human STRING database (12, 13). To avoid false positive interactions, a Stepminer-derived cutoff of combined interaction score was selected (12, 13). A complete list of edges is provided in **Supplemental Information 1**.

Once constructed, the network was perturbed using two approaches. First, an *in-silico* deletion of ELMO1 was performed, and each node within this perturbed network (without ELMO1) was assessed for the following

network metrics: (i) Betweenness centrality, (ii) Closeness centrality, and (iii) Shortest Path Alteration Fraction (SPAF) (14). Difference in Z score, ∆Z, of each node, N, for each of the above mentioned topological metrices was calculated. Proteins with ∆Z >0.1 were identified as those that were impacted due to the deletion of ELMO1.

As a second approach, an *in-silico* deletion of ELMO1•SifA interaction(edge) was performed, and each edge within this perturbed network (without ELMO1•SifA edge) was assessed for two independent metrices: (i) Edge betweenness centrality and (ii) Edge Proximity (15). Edges with ∆Z >0.1 were identified as those that were impacted due to the selective deletion of the ELMO1•SifA interaction.

A group of proteins that are impacted, as determined by at least more than one topological node-based metrices, or either of the two edge-based metrics, were used for KEGG enrichment analysis (using ShinyGO v0.76; http://bioinformatics.sdstate.edu/go/). All the codes for network analysis are available at https://github.com/sinha7290/ELMO.

Measurement of Rac1 activity

ELMO1-depleted murine J774 macrophage cell lines were transfected with ELMO1 WT and ELMO1 K3D plasmids and infected with *Salmonella enterica* serovar Typhimurium for 15 and 30 min (MOI 1:50) and Rac1 activity was measured by pull-down assay using a commercial kit. First, infected cells were lysed with the lysis buffer provided in the kit. Equal aliquots of cell lysates (~ 800 µg total cell protein) were added to 10 µg (10 µl) of immobilized GST-PBD (glutathione *S*-transferase with p21-binding domain of Pak1) (a.k.a., PAK-PBD beads) and incubated at 4°C on a rotator for 1 h. PAK-PBD beads were recovered by centrifugation at 5,000 x g at 4°C. Unbound lysates were removed and the beads were washed once with 500 µl Wash Buffer prior to eluting the proteins with 20 µl of 2x Laemmli sample buffer and boiling for 5 min at 100°C. Input lysates and eluates from the PAK-PBD beads were resolved on a 12.5% SDS-PAGE, and transferred for 45 min, followed by quantitative immunoblotting.

Bacterial internalization assays

Approximately $0.5*10^6$ ELMO1-depleted murine macrophage cells were seeded into 12-well culture dishes ~12 h before transfection with either FLAG-ELMO1 WT or FLAG-ELMO1 K3D. After 48 hours of transfection, cells were infected with SL at a MOI of 1:50 for 30 min in antibiotic free media. The cells were then washed and incubated with gentamicin (500 mg/ml) for 90 min to kill the extracellular bacteria. Subsequently, the cells were lysed in 1% Triton-X100, and the lysates were serially diluted and plated directly onto Luria-Bertani agar plates. The total colony-forming units (CFUs) were enumerated the next day after overnight incubation of the plates at 37°C.

Image Processing

All images were processed on ImageJ software (NIH) or iStudio (LiCOR) software and assembled into figure panels using Photoshop and Illustrator (Adobe Creative Cloud). All graphs were generated using GraphPad Prism v9.3.1.

QUANTIFICATION AND STATISTICAL ANALYSIS

Statistical Analysis and Replicates

All experiments were repeated at least three times, and results were presented as average ± S.E.M. Statistical significance was assessed using either t-test or one-way analysis of variance (ANOVA) including a Tukey's test for multiple comparisons. Actual *p* values are displayed.

Supplementary Figures and Legends

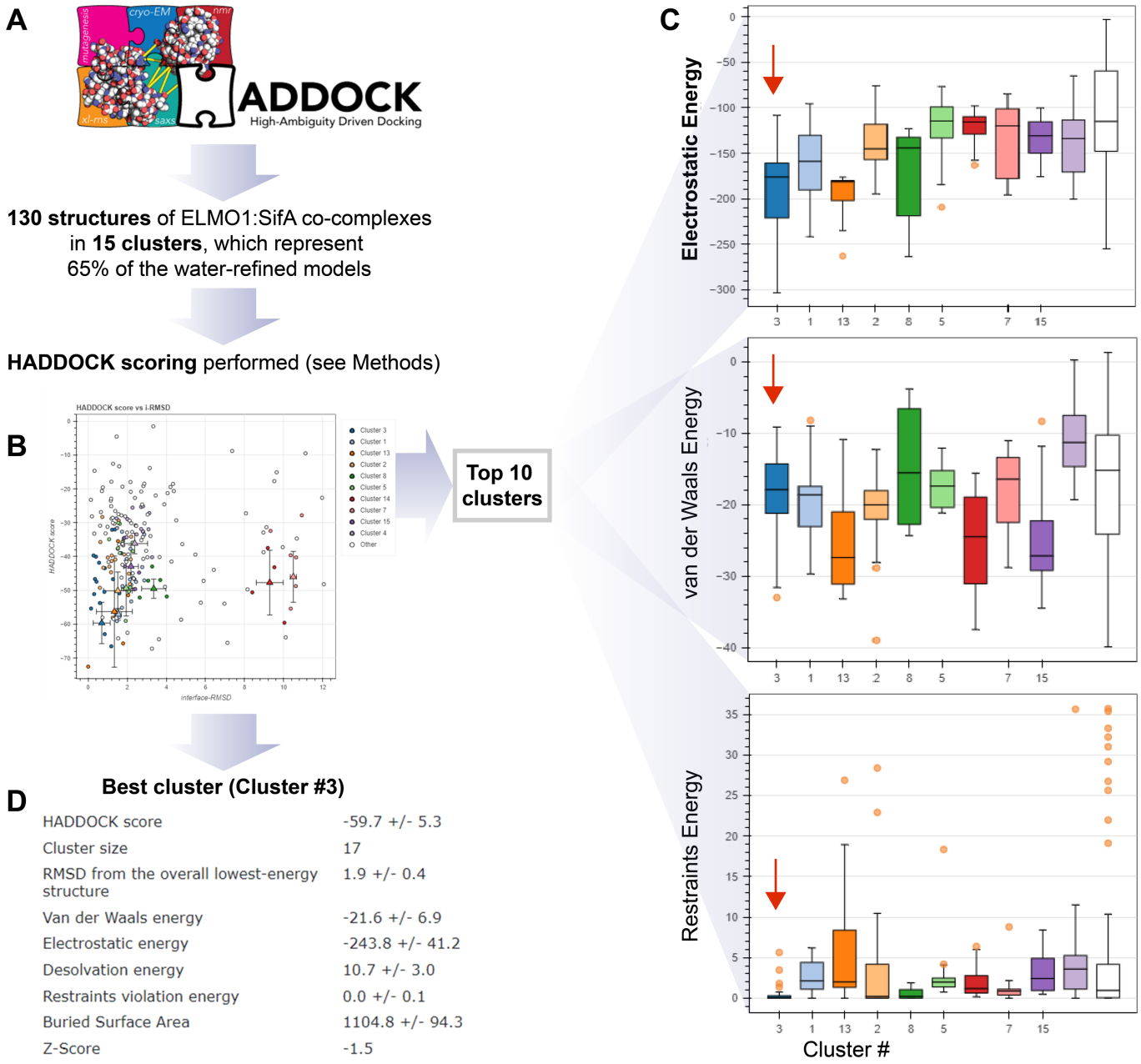

Supporting figure S1 [Related to Figure 2]: The workflow for the creation and analysis of the homology model of the ELMO1•SifA co-complex.

A. HADDOCK (High Ambiguity Driven protein-protein DOCKing) [HADDOCK2.4 web server HADDOCK Web Server (uu.nl)] is used for analyzing ELMO1•SifA interaction, which revealed several possible structures of the co-complex.
B. HADDOCK scoring is performed according to the weighted sum HADDOCK score of various parameters (HADDOCK2.2 scoring function; see Methods).
C-D. Key properties [Electrostatic, top; van der Waals, middle; and restraints energy, bottom] of the top 10 clusters are shown as whisker plots. Red → marks the properties of the best cluster (based on parameters shown in D). Cluster 3 models were chosen for further analysis based on the Z-score (-1.5; see panel D), which indicates how many standard deviations from the average this cluster is in terms of score (the more negative the better). Results indicate strong electrostatic energy as a major parameter contributing to the selection of the cluster for the formation and/or stabilization of the co-complex.

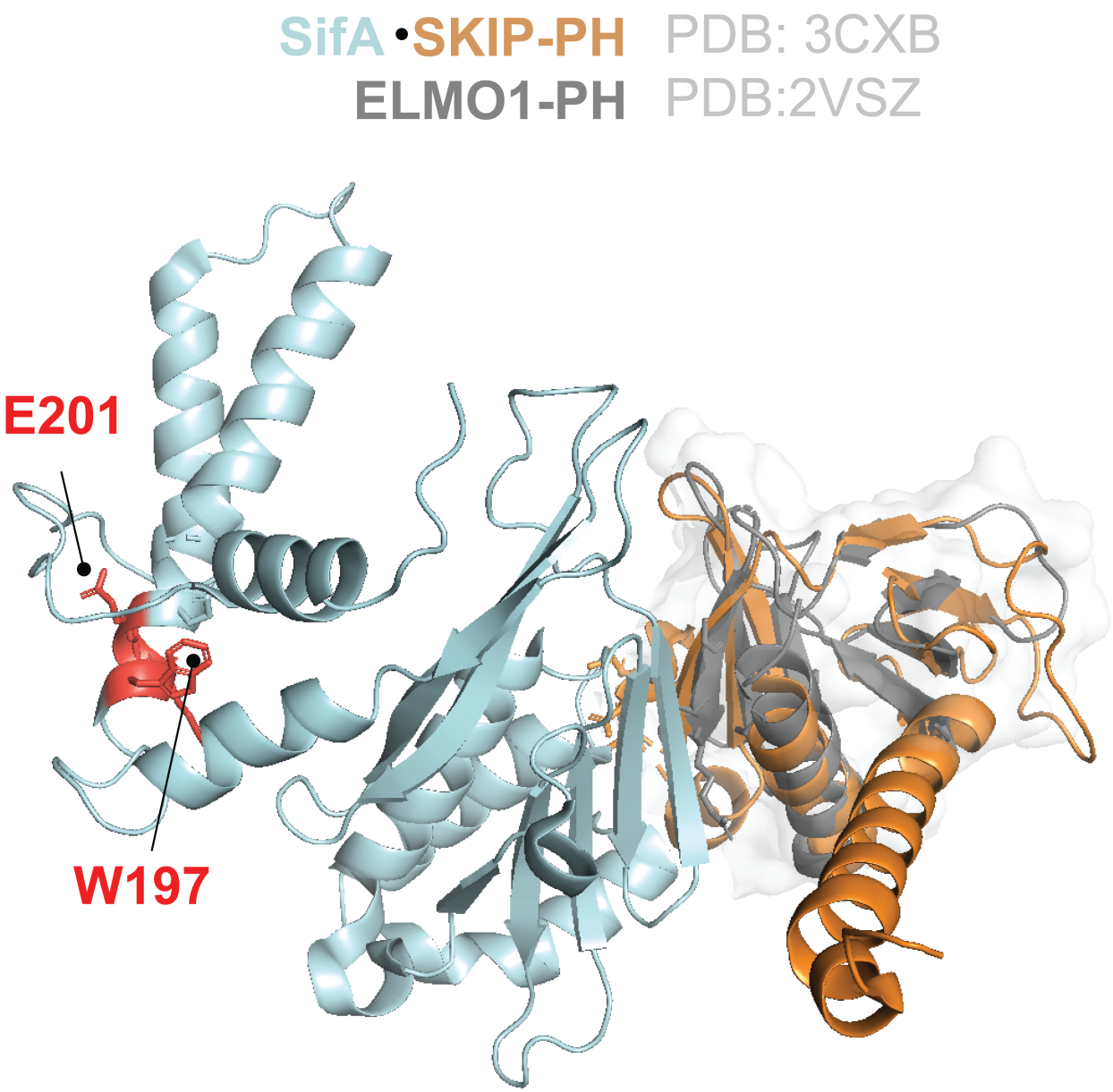

Supporting figure S2 [Related to Figure 2]: W197 and E201 in *W*xxx*E* motif in SifA is not predicted to participate in the ELMO1•SifA interaction.

Homology model of the ELMO1(gray)•SifA(turquoise) complex, generated by superimposing the solved structure of the ELMO1-PH (PDB:2VSZ) on that of the SKIP-PH (golden) in complex with SifA (PDB:3CXB). The executive root mean square deviation (RMSD) of the model is 1.528. The tryptophan (W) and glutamate (E) within the WxxxE-motif in SifA are highlighted in red.

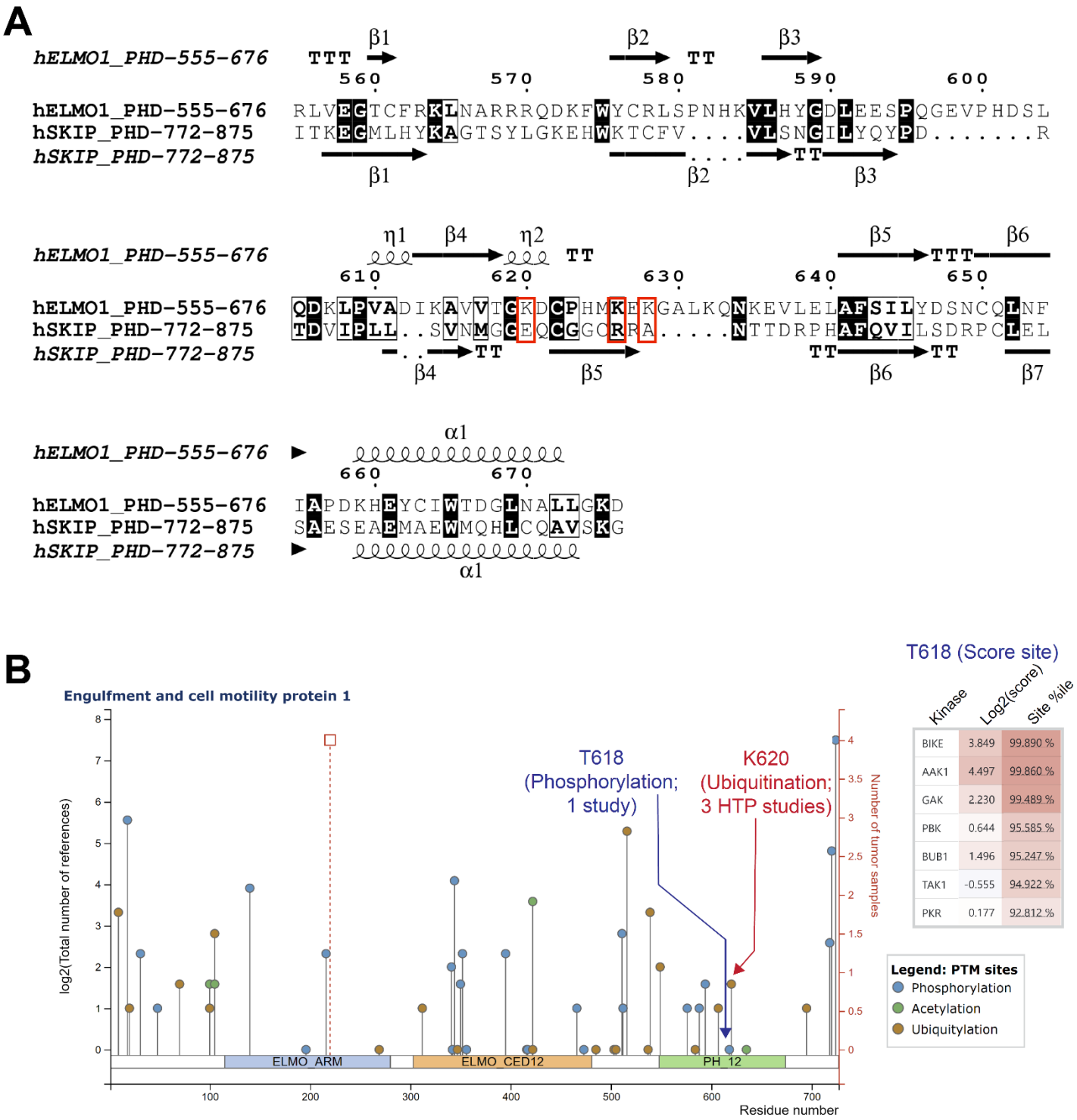

Supporting figure S3 [Related to Figure 2]: A polar lysine triad on ELMO1 binds SifA.

A: An alignment of the sequence corresponding to the PH domains of ELMO1, and SKIP is shown, along with secondary structures. Conserved residues are shaded in black, similar residues in gray box. Three lysine residues on ELMO1 were identified as critical for binding with SifA are marked with red box and were mutated in this work to confirm that they are essential for the ELMO1-SifA interaction.

B. Post-translational modifications identified at or near the lysine triad is shown, as curated at phosphosite.org (https://www.phosphosite.org/homeAction). K620 is ubiquitinated, whereas T618 is phosphorylated. No disease-causing SNPs or somatic mutations were found to directly impact the lysine triad.

```
MULTIPLE SEQUENCE ALIGNMENT

Human_ELMO1_AF398885.1        541------------QPEILELIKQQRLNRLVEGTCFRKLNARRRQDKFWYCRLSPNHKV
Chimp_ELMO1_XM_009452903.3    541--RPILELKEKIQPEILELIKQQRLNRLVEGTCFRKLNARRRQDKFWYCRLSPNHKV
Cow_ELMO1_NM_001113227.2      541------------QPEILELIKQQRLNRLVEGTCFRKLNCRRRQDKFWYCRLSPNHKV
Horse_ELMO1_XM_023639524.1    541--RPILELKEKIQPEILELIKQQRLNRLVEGTCFRKLNCRRRQDKFWYCRLSPNHKV
Pig_ELMO1_XM_021079240.1      541------------QPEILELIKQQRLNRLVEGTCFRKLNCRRRQDKFWYCRLSPNHKV
Mouse_ELMO1_AF398883.1        541------------QPEILELIKQQRLNRLVEGTCFRKLNARRRQDKFWYCRLSPNHKV
Rat_ELMO1_NM_001395578.1      541------------QPEILELIKQQRLNRLVEGTCFRKLNARRRQDKFWYCRLSPNHKV
Z-fish_ELMO1_XM_009294309.3   541--RPILELREKIQPEIMELIKQQRLNRLCEGTCFRKISSRRRQDKFWYCRLSPNHKV
Zenopus_ELMO1_XM_018095011.2  541------------QPEIIELIKQQRLNRLVEGTCFRKLNSRRRQDKFWYCRLSPNHKV

Human_ELMO2_AF398886.1        541--------------------IKQQRLNRLCEGSSFRKIGNRRRQERFWYCRLALNHKV
Human_ELMO3_NM_024712.5       541------------------------------LRLCEGTLFRKISSRRRQDKLWFCCLSPNHKL
                                                                ** **: ***:. ****:::*:* *: ***:

                                                                          ▼   ▼▼
Human_ELMO1_AF398885.1        LHYGDLEESPQGEVPHDSLQDKLPVADIKAVVTGKDCPHMKEKGALKQNKEVLELAFSIL
Chimp_ELMO1_XM_009452903.3    LHYGDLEESPQGEVPHDSLQDKLPVADIKAVVTGKDCPHMKEKGALKQNKEVLELAFSIL
Cow_ELMO1_NM_001113227.2      LHYGDLEESPQGEVPHDSLQDKLPVADIKAVVTGKDCPHMKEKGALKQNKEVLELAFSIL
Horse_ELMO1_XM_023639524.1    LHYGDLEESPQGEVPHDSLQDKLPVADIKAVVTGKDCPHMKEKGALKQNKEVLELAFSIL
Pig_ELMO1_XM_021079240.1      LHYGDLEESPQGEVPHDSLQDKLPVADIKAVVTGKDCPHMKEKGALKQNKEVLELAFSIL
Mouse_ELMO1_AF398883.1        LHYGDLEESPQGEVPHDSLQDKLPVADIKAVVTGKDCPHMKEKGALKQNKEVLELAFSIL
Rat_ELMO1_NM_001395578.1      LHYGDLEESPQGEVPHDSLQDKLPVADIKAVVTGKDCPHMKEKGALKQNKEVLELAFSIL
Z-fish_ELMO1_XM_009294309.3   LHYGDLEESPQGEVPHDSLQDKLPVADIKAVVTGKDCPHMKEKGALKQNKEVLELAFSVL
Zenopus_ELMO1_XM_018095011.2  LHYGDLEESPQGEVPHDSLQDKLPVADIKAIVTGKDCPHMKEKGALKQNKEVLELAFSIM

Human_ELMO2_AF398886.1        LHYGDLDDNPQGEVTFESLQEKIPVADIKAIVTGKDCPHMKEKSALKQNKEVLELAFSIL
Human_ELMO3_NM_024712.5       LQYGDMEEGAS-PPTLESLPEQLPVADMRALLTGKDCPHVREKGSGKQNKDLYELAFSIS
                              *:***:::. .     :** :::****::*::*******::**.: ****:: *****:

Human_ELMO1_AF398885.1        YDSN---CQLNFIAPDKHEYCIWTDGLNALLGKDMMSDLTRNDLDTLLSMEIKLRLLDLE
Chimp_ELMO1_XM_009452903.3    YDSN---CQLNFIAPDKHEYCIWTDGLNALLGKDMMSDLTRNDLDTLLSMEIKLRLLDLE
Cow_ELMO1_NM_001113227.2      YDSN---CQLNFIAPDKHEYCIWTDGLNALLGKDMMSDLTRNDLDTLLSMEIKLRLLDLE
Horse_ELMO1_XM_023639524.1    YDSN---CQLNFIAPDKHEYCIWTDGLNALLGKDMMSELTRNDLDTLLSMEIKLRLLDLE
Pig_ELMO1_XM_021079240.1      YDSN---CQLNFIAPDKHEYCIWTDGLNALLGKDMMSDLTQNDLDTLLSMEIKLRLLDLE
Mouse_ELMO1_AF398883.1        YDSN---CQLNFIAPDKHEYCIWTDGLNALLGKDMMSDLTRNDLDTLLSMEIKLRLLDLE
Rat_ELMO1_NM_001395578.1      YDSN---CQLNFIAPDKHEYCIWTDGLNALLGKDMMSDLTRNDLDTLLSMEIKLRLLDLE
Z-fish_ELMO1_XM_009294309.3   YESD---EYLNFIAPDKHEYCVWTDGLNALLGKEMSSEFTRSDMDTLLNMEMKLRLLDLE
Zenopus_ELMO1_XM_018095011.2  YDSN---CQLNFIAPDKHEYCIWTDGLNALLGKDMISDLTRNDMDTLLSMELKLRLLDLE

Human_ELMO2_AF398886.1        YDPD---ETLNFIAPNKYEYCIWIDGLSALLGKDMSSELTKSDLDTLLSMEMKLRLLDLE
Human_ELMO3_NM_024712.5       YDRGEEEAYLNFIAPSKREFYLWTDGLSALLGSPMGSEQTRLDLEQLLTMETKLRLLELE
                              *: .     ******.* *: :* ***.****. * *: *: *:: **.** *****:**

Human_ELMO1_AF398885.1        NIQIPDAPPPIPKEPSNYDFVYDCN----  727
Chimp_ELMO1_XM_009452903.3    NIQIPDAPPPIPKEPSNYDFVYDCN----  742
Cow_ELMO1_NM_001113227.2      NIQIPDAPPPIPKEPSNYDFVYDCN----  727
Horse_ELMO1_XM_023639524.1    NIQIPDAPPPIPKEPSNYDFVYDCN----  742
Pig_ELMO1_XM_021079240.1      NIQIPDAPPPIPKEPSNYDFVYDCN----  727
Mouse_ELMO1_AF398883.1        NIQIPDAPPPIPKEPSNYDFVYDCN----  727
Rat_ELMO1_NM_001395578.1      NIQIPDAPPPIPKEPSNYDFVYDCN----  727
Z-fish_ELMO1_XM_009294309.3   NIQIPEVPPPIPKEPSNYDFVYDCN----  740
Zenopus_ELMO1_XM_018095011.2  NIQIPDAPPPIPKEPSNYDFVYDCN----  727

Human_ELMO2_AF398886.1        NIQIPEAPPPIPKEPSSYDFVYHYG----  720
Human_ELMO3_NM_024712.5       NVPIPERPPPVPPPPTNFNFCYDCSIAEP  720
                              *: **: ***:*  *:.::* *. .
```

Supporting figure S4 [Related to Figure 2]: The basic 'patch' in the β5-β6 loop within the PH domain, and the triad of lysines that are predicted to bind SifA, are evolutionarily conserved in ELMO1.

A sequence alignment of the ELMO1 PH domain region and C-terminal residues from various species, as well as the human ELMO2 and ELMO3 isoforms is shown. Green boxes indicate the previously determined DOCK180-binding sites(16); red solid box within the green box indicates the canonical 'PxxP'-motif, which is the SH3 domain binding site. The β5- β6 loop region is highlighted with a red lined box. Black arrowheads highlight the three lysine (K) residues that were predicted and validated as important residues for binding SifA.

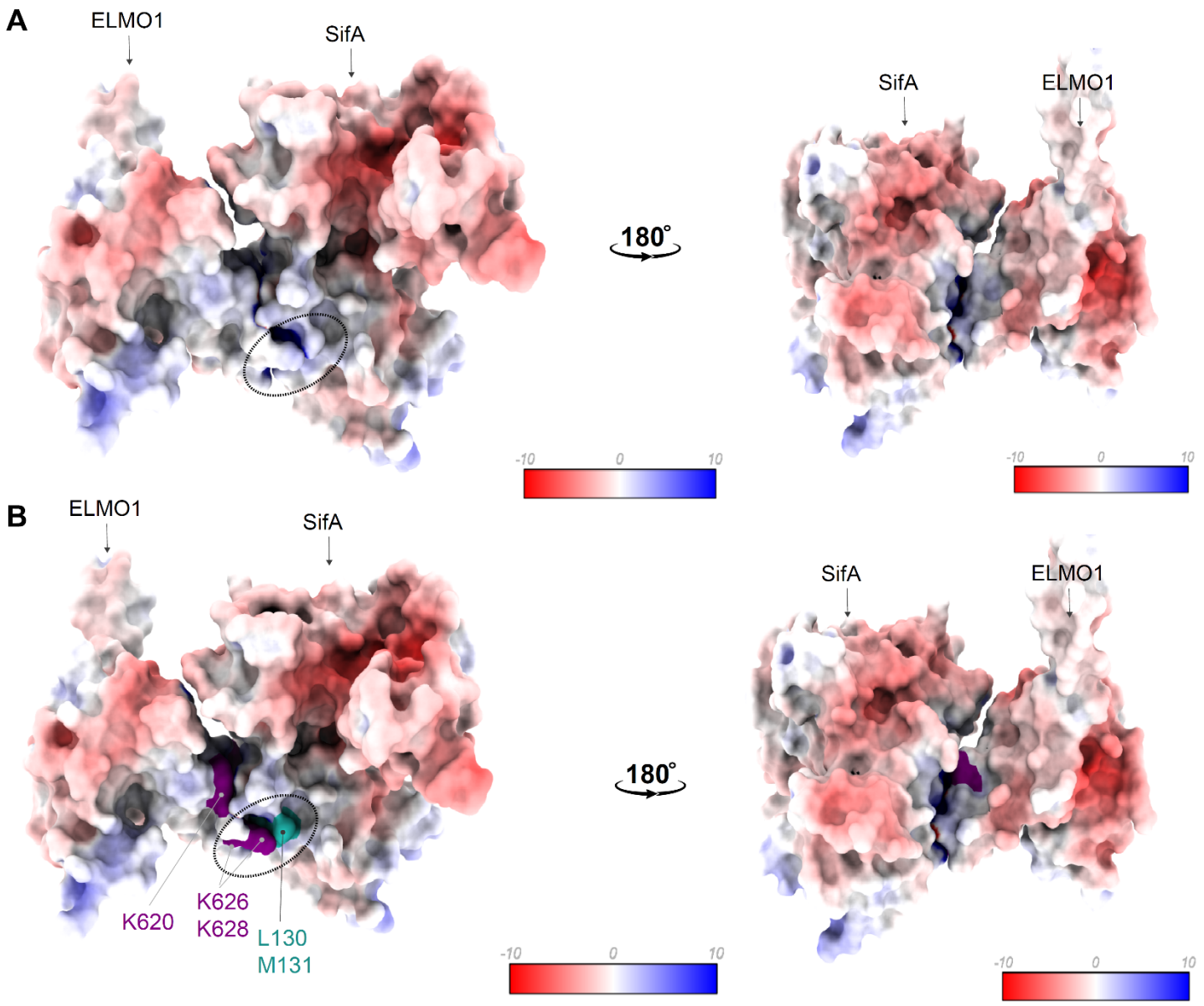

Supporting figure S5 [Related to Figure 2]: APBS (Adaptive Poisson-Boltzmann Solver)-derived surface electrostatics of the ELMO1•SifA co-complex.

Electrostatic surface potential (kT/e) for an all-side chain model of the ELMO1•SifA co-complex, calculated using adaptive Poisson-Boltzmann solver (APBS), an NIH-supported software (9) [https://www.poissonboltzmann.org/] for the estimation of electrostatic forces for large bimolecular assemblages. Panels display APBS output data, as visualized using Chimaera. Volume surface coloring was set in the default range of -10 (red), through 0 (white), to +10 (blue) kT/e, where negatively charged surfaces are red (-10 kT/e) and positively charged surfaces are blue (+10 kT/e). Top (unlabeled; **A**) and bottom (labeled; **B**) panels show the same co-complex, from two directions (left- and right-side views). In the most energetically favorable orientation, charged residues Lys(K)628 and Lys(K)626 on (ELMO1) bring hydrophobic residues Met(M)131 and Leu(L)130 on SifA into proximity [marked by an oval].

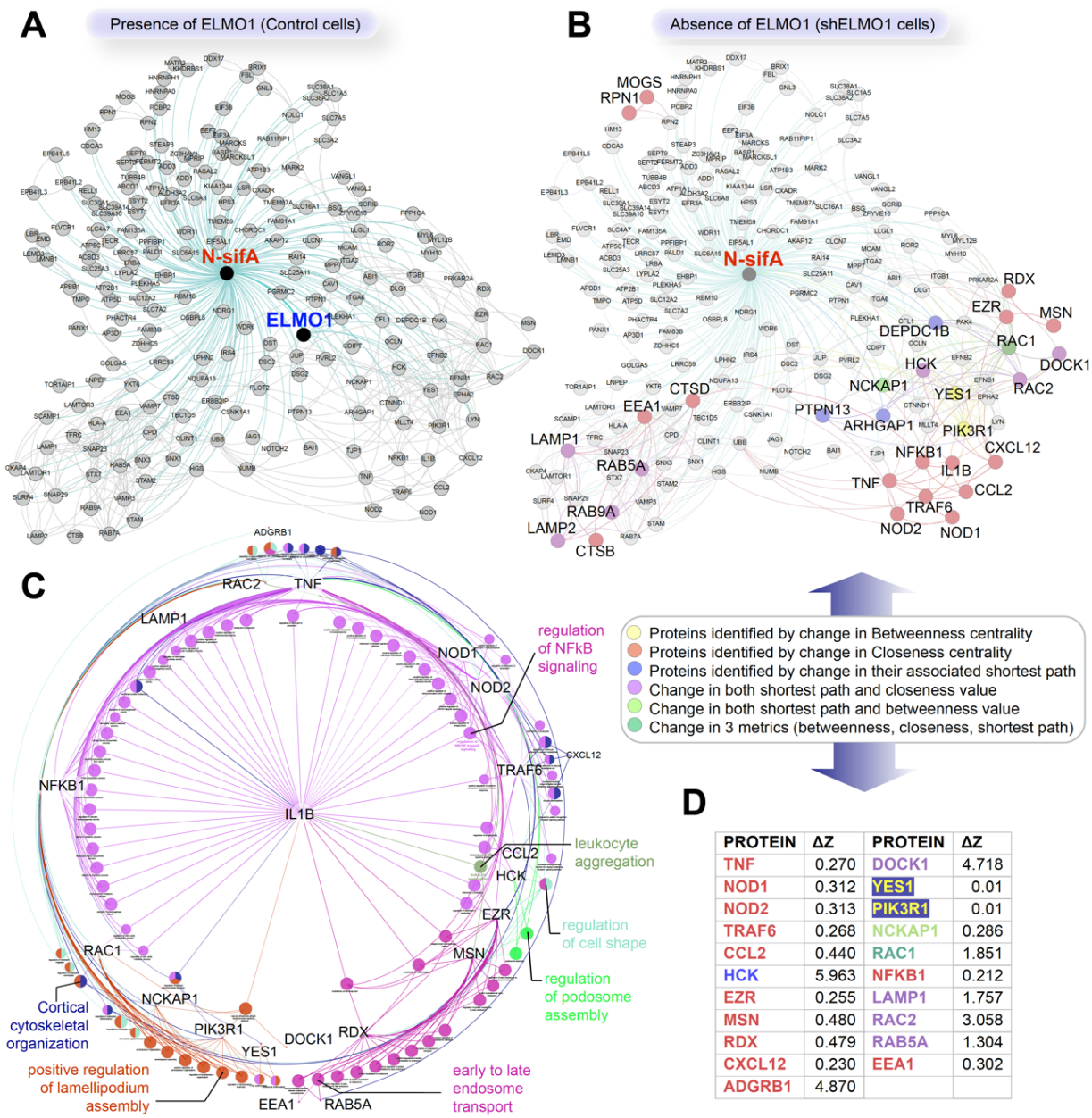

PROTEIN	ΔZ	PROTEIN	ΔZ
TNF	0.270	DOCK1	4.718
NOD1	0.312	YES1	0.01
NOD2	0.313	PIK3R1	0.01
TRAF6	0.268	NCKAP1	0.286
CCL2	0.440	RAC1	1.851
HCK	5.963	NFKB1	0.212
EZR	0.255	LAMP1	1.757
MSN	0.480	RAC2	3.058
RDX	0.479	RAB5A	1.304
CXCL12	0.230	EEA1	0.302
ADGRB1	4.870		

Supporting figure S6 [Related to Figure 3]: Prediction of cellular consequences of depletion of ELMO1 by *in-silico* perturbation of protein-protein interaction networks.

A. A protein-protein interaction (PPI) network of *SifA* and its human interactome was constructed by leveraging a previously published proximity labeling (BioID) study(2) that mapped the SifA-interactome to fetch the remaining host interactors of the SifA-interactome using the STRING database. The ELMO1●*SifA* interaction, which is the focus of current study, is highlighted. See also **Figure 3A** for workflow.

B. *Top*: A PPI network as in A, but in the absence of ELMO1 with a consequent loss of its interactions. The colored nodes highlight the topological effect of network perturbation by ELMO1 deletion, as determined by differential analysis of standard topological metrics, e.g., Betweenness, Closeness and shortest path alteration fractions. *Bottom*: A key with color code is presented.

C. Graph displays the pathway enrichment analysis of the identified proteins in B, determined using the ClueGO algorithm. Pathways with significant alterations are highlighted.

D. Table displays a selected list of proteins that display the greatest change in each metric, summarized as changes in Z scores. Changes > 0.1 are listed. See also **Figure 3B-C** for further analysis and interpretation.

```
SIFA_S. ENTERICA       MPITIGNGFLKSEILTNSPRNTKEAWWKVLWEKIKDFFFSTGKAKADRCLHEMLFAERAP  60
SIFB_S. ENTERICA       MPITIGRGFLKSEMFSQSAI-SQRSFFTLLWERIKDFFCDTQRSTADQYIKELCDVASPP  59
IPGB1_S. FLEXNERI      ------------------------------------------------------------  0
IPGB2_S. FLEXNERI      ------------------------------------------------------------  0
MAP_E. COLI            ------------------------------------------------------------  0
ESPM_E. COLI           ------------------------------------------------------------  0
ESPT_C. RODENTIUM      ------------------------------------------------------------  0

SIFA_S. ENTERICA       TRERLTEIFFELKELACASQRDRFQVHNPHENDATIILRIMDQNEENELLRITQNTDTFS  120
SIFB_S. ENTERICA       DAQRLFDLFCALYELSSPSCRGNFHFQHYKDAECQYTNLFIKD-GEDIPLCIVIRQDHYY  118
IPGB1_S. FLEXNERI      ------------------------------------------------------------  0
IPGB2_S. FLEXNERI      ------------------------------------------------------------  0
MAP_E. COLI            ------------------------------------------------------------  0
ESPM_E. COLI           ------------------------------------------------------------  0
ESPT_C. RODENTIUM      ------------------------------------------------------------  0

                                 ⬇⬇
SIFA_S. ENTERICA       CEVMGNLYFLMKDRPDILKSHPQMTAMIKR-----------------RYSEIVDYPLPST  163
SIFB_S. ENTERICA       YD-------IMNRTVLCVDTQPAHLKRYSDITIKAST----------YVCEELCCLFPER  161
IPGB1_S. FLEXNERI      ----MQILNKILP---------QVEFAIPRPSFDSLSHNKLVKKILSVFNLKQRFP----  43
IPGB2_S. FLEXNERI      ---------------MLGTSFNNFGISLSH----K-RYFS------GKVDEIIRCT----  30
MAP_E. COLI            ------MFSPMT---MAGRSLVQATAQTLRPAVTRAAMQA------GTGATGMRFM----  41
ESPM_E. COLI           --------MPMN---TTGTSFSSFGISCHRENSFR-NSFL------GKNDEVIKCS----  38
ESPT_C. RODENTIUM      --------MPGT------ISSSGFGFSIAK----Q-PHSS------GQKTVIDGFF----  31

SIFA_S. ENTERICA       LCLNPAGAPILSVPLDNIEGYLYTE----LRKGHLDGWKAQEKATYLAAKIQSGIEKTTR  219
SIFB_S. ENTERICA       LLLSLSGGITFPVDLKNIKETLIAM----AEKGNLCDWKEQERKAAISSRINLGIAQADV  217
IPGB1_S. FLEXNERI      -----QKNFGCPVNINKIRDSVIDKIKDSNSGNQLFGWMSQERTSYVSSMINRSIDEMAI  98
IPGB2_S. FLEXNERI      -----MGKRIVKISSTKINTSILSSVSEQ-IGENITDWKNDEKKVYVSRVVNQCIDKFCA  84
MAP_E. COLI            -----PVQSNFVINHGKLTNQLLQAVAKQTRNGDTQGWFQQEQTTYISRTVNRTLDDYCR  96
ESPM_E. COLI           -----MGERTIHFSVRKFSGNILDTVNRQ-NTKDINGWIKDERIVYPSRVINQEIDNYCF  92
ESPT_C. RODENTIUM      -----LGTRKISFSYLRLESELMQCINLK-NEGKMNEWMREECICFVSRDVNKQLDIFAK  85
                                   .   .:   :           .   *  :*     :  ::  :

SIFA_S. ENTERICA       ILHHANISESTQQNAFLETMAMCGLKQLEIPPPHTHIPIEKMVKEVLLADKTFQAFLVTD  279
SIFB_S. ENTERICA       PPIDDAIKNKI----AAKVIENTNLKNAAFEPNYAQSSVTQIVYSCLFKNEILMNMLEES  273
IPGB1_S. FLEXNERI      -HNGVVLTSDNKKNIFAAIEKKF--PDIKLDEKSAQTSISHTALNEIASSGLRAKILKRY  155
IPGB2_S. FLEXNERI      -EHSRKIGDNLRKQIFKQVEKDY---RISLDINAAQSSINHLVSGSSYFKKKMDELCEGM  140
MAP_E. COLI            -SNNSVISKETKGHIFRAVENAL---QQPLDMNGAQSSIGHFLQSNKYFNQKVDEQCGKR  152
ESPM_E. COLI           -QKNAKISTEERQRVFSLVSHRY---QLTLDVKAAQSSINHVIMGNASFGKKIDTLCDSM  148
ESPT_C. RODENTIUM      -NNQTTIPGCVRERVFQRASFHC---GFSLDVRCAQTSTHHMILNSLYFQKKMDTLFGSA  141
                             :                     :    ::    :

SIFA_S. ENTERICA       P--STS-QSMLAEIVEAISDQVFHAIFRIDPQAIQKMAEEQLTTLHVRSEQQSGCLCCFL  336
SIFB_S. ENTERICA       S--FHG-LLCLNELTEYVALQVHNSLFSEDLSSLVETTK---NEAHH----QS-------  316
IPGB1_S. FLEXNERI      SSDMDLFNTQMKDLTNLVSSSVYDKIFNESTKVLQIEISAEVLKAVYRQSNTN-------  208
IPGB2_S. FLEXNERI      NRSVKN-DTT-SNVANLISDQFFEKNVQ-YIDLKKLR--GNMSDYITNLESPF-------  188
MAP_E. COLI            VDPITRFNTQ-TKMIEQVSQEIFERNFSG-FKVSEIK-------AITQNA----------  193
ESPM_E. COLI           SRDVKN-RTA-DCIANSLADKFYQKHIEPDIDIVKLR--NEIPDYLRCTIQA--------  196
ESPT_C. RODENTIUM      DVEVRN-QCV-RTALSSLADIFFERNVN-SIDMNKFR--DKVYDAIVQEAQRT-------  189
                                 . ::  ...  .    .
```

Supporting figure S7 [Related to Figure 4]:

The WxxxE-motif containing effector proteins have divergent sequences and the L130/M131 residues on SifA that bind ELMO1 are not conserved.

Multiple sequence alignment of IpgB1 [AY206439.1] and IpgB2 [AY879342.1] from Shigella flexneri, EspM [BHZP01000031.1] and Map [WP_150349845.1] from enteropathogenic E. coli, EspT [FM210026.1[from C. rodentium, and SifA [AAA97467.1] and SifB [AF128839.1] from Salmonella enterica serovar typhimurium. The WxxxE motif (blue box) and the catalytic loop (magenta box) that was previously determined(17) as critical for the activation of small GTPases of the Rho/ family are highlighted.

Supplementary references

1. Das, S., Sarkar, A., Choudhury, S. S., Owen, K. A., Castillo, V., Fox, S. *et al.* (2015) ELMO1 has an essential role in the internalization of Salmonella Typhimurium into enteric macrophages that impacts disease outcome Cell Mol Gastroenterol Hepatol **1**, 311-324 10.1016/j.jcmgh.2015.02.003
2. D'Costa, V. M., Coyaud, E., Boddy, K. C., Laurent, E. M. N., St-Germain, J., Li, T. *et al.* (2019) BioID screen of Salmonella type 3 secreted effectors reveals host factors involved in vacuole positioning and stability during infection Nat Microbiol **4**, 2511-2522 10.1038/s41564-019-0580-9
3. Steele-Mortimer, O., Brumell, J. H., Knodler, L. A., Méresse, S., Lopez, A., andFinlay, B. B. (2002) The invasion-associated type III secretion system of Salmonella enterica serovar Typhimurium is necessary for intracellular proliferation and vacuole biogenesis in epithelial cells Cell Microbiol **4**, 43-54 10.1046/j.1462-5822.2002.00170.x
4. Stein, M. A., Leung, K. Y., Zwick, M., Garcia-del Portillo, F., andFinlay, B. B. (1996) Identification of a Salmonella virulence gene required for formation of filamentous structures containing lysosomal membrane glycoproteins within epithelial cells Mol Microbiol **20**, 151-164 10.1111/j.1365-2958.1996.tb02497.x
5. Das, S., Sarkar, A., Choudhury, S. S., Owen, K. A., Castillo, V., Fox, S. *et al.* (2015) ELMO1 has an essential role in the internalization of Typhimurium into enteric macrophages that impacts disease outcome Cell Mol Gastroenterol Hepatol **1**, 311-324 10.1016/j.jcmgh.2015.02.003
6. den Hartog, G., Butcher, L. D., Ablack, A. L., Pace, L. A., Ablack, J. N. G., Xiong, R. *et al.* (2021) Apurinic/Apyrimidinic Endonuclease 1 Restricts the Internalization of Bacteria Into Human Intestinal Epithelial Cells Through the Inhibition of Rac1 Front Immunol **11**, 553994-553994 10.3389/fimmu.2020.553994
7. Das, S., Owen, K. A., Ly, K. T., Park, D., Black, S. G., Wilson, J. M. *et al.* (2011) Brain angiogenesis inhibitor 1 (BAI1) is a pattern recognition receptor that mediates macrophage binding and engulfment of Gram-negative bacteria Proceedings of the National Academy of Sciences of the United States of America **108**, 2136-2141 10.1073/pnas.1014775108
8. de Vries, S. J., van Dijk, M., andBonvin, A. M. (2010) The HADDOCK web server for data-driven biomolecular docking Nat Protoc **5**, 883-897 10.1038/nprot.2010.32
9. Jurrus, E., Engel, D., Star, K., Monson, K., Brandi, J., Felberg, L. E. *et al.* (2018) Improvements to the APBS biomolecular solvation software suite Protein Sci **27**, 112-128 10.1002/pro.3280
10. Pettersen, E. F., Goddard, T. D., Huang, C. C., Couch, G. S., Greenblatt, D. M., Meng, E. C. *et al.* (2004) UCSF Chimera--a visualization system for exploratory research and analysis J Comput Chem **25**, 1605-1612 10.1002/jcc.20084
11. Szklarczyk, D., Gable, A. L., Nastou, K. C., Lyon, D., Kirsch, R., Pyysalo, S. *et al.* (2021) The STRING database in 2021: customizable protein-protein networks, and functional characterization of user-uploaded gene/measurement sets Nucleic Acids Res **49**, D605-D612 10.1093/nar/gkaa1074
12. Sahoo, D., Seita, J., Bhattacharya, D., Inlay, M. A., Weissman, I. L., Plevritis, S. K. *et al.* (2010) MiDReG: a method of mining developmentally regulated genes using Boolean implications Proc Natl Acad Sci U S A **107**, 5732-5737 10.1073/pnas.0913635107
13. Qiao, L., Sinha, S., Abd El-Hafeez, A. A., Lo, I. C., Midde, K. K., Ngo, T. *et al.* (2023) A circuit for secretion-coupled cellular autonomy in multicellular eukaryotic cells Mol Syst Biol e11127 10.15252/msb.202211127
14. Sinha, S., Samaddar, S., Das Gupta, S. K., andRoy, S. (2021) Network approach to mutagenesis sheds insight on phage resistance in mycobacteria Bioinformatics 10.1093/bioinformatics/btaa1103
15. Banerjee, S. J., Sinha, S., andRoy, S. (2015) Slow poisoning and destruction of networks: edge proximity and its implications for biological and infrastructure networks Phys Rev E Stat Nonlin Soft Matter Phys **91**, 022807 10.1103/PhysRevE.91.022807
16. Komander, D., Patel, M., Laurin, M., Fradet, N., Pelletier, A., Barford, D. *et al.* (2008) An alpha-helical extension of the ELMO1 pleckstrin homology domain mediates direct interaction to DOCK180 and is critical in Rac signaling Mol Biol Cell **19**, 4837-4851 10.1091/mbc.e08-04-0345
17. Bulgin, R., Raymond, B., Garnett, J. A., Frankel, G., Crepin, V. F., Berger, C. N. *et al.* (2010) Bacterial guanine nucleotide exchange factors SopE-like and WxxxE effectors Infect Immun **78**, 1417-1425 10.1128/iai.01250-09